Spatial patterns of ectoenzymatic kinetics in relation to biogeochemical properties in the Mediterranean Sea and the concentration of the fluorogenic substrate used.

France Van Wambeke[1], Elvira Pulido[1], Philippe Catala[3], Julie Dinasquet[2,3], Kahina Djaoudi[1,4], Anja Engel[5], Marc Garel[1], Sophie Guasco[1], Barbara Marie[3], Sandra Nunige[1], Vincent Taillandier[6], Birthe Zäncker[6,7], Christian Tamburini[1].

[1]Aix-Marseille Université, CNRS/INSU, Université de Toulon, IRD, Mediterranean Institute of Oceanography (MIO) UM 110, 13288, Marseille, France
[2]Marine Biology Research Division, Scripps Institution of Oceanography, UCSD, La Jolla, USA
[3]Sorbonne Universités, UPMC University Paris 6, Laboratoire d'Océanographie Microbienne (LOMIC), Observatoire Océanologique, 66650, Banyuls/mer
[4]Molecular and Cellular Biology, The University of Arizona, Tucson, USA
[5]GEOMAR – Helmholtz-Centre for Ocean Research, Kiel, Germany
[6]CNRS, Sorbonne Universités, Laboratoire d'Océanographie de Villefranche (LOV), UMR7093, 06230 Villefranche-sur-Mer, France
[7]The Marine Biological Association of the UK, Plymouth, United Kingdom

Correspondence to: F. Van Wambeke (france.van-wambeke@mio.osupytheas.fr)

Abstract. Ectoenzymatic activity, prokaryotic heterotrophic abundances and production were determined in the Mediterranean Sea. Sampling was carried out in the sub surface, the deep chlorophyll maximum layer, the core of the Levantine Intermediate waters and in the deeper part of the mesopelagic layers. Michaelis-Menten kinetics were assessed, using a large range of concentrations of fluorogenic substrates (0.025 to 50 µM). As a consequence, Km and Vm parameters were determined for both low and high affinity enzymes for alkaline phosphatase, aminopeptidase and β−glucosidase. Based on the constant derived from the high LAP affinity enzyme (derived from a 0.025-1 µM range of concentrations), *in-situ* hydrolysis of N-protein contributed of 48% ± 30% to the heterotrophic bacterial nitrogen demand within the epipelagic layers and of 180% ± 154% below (in the Levantine Intermediate waters and the upper part of the mesopelagic layers). The LAP hydrolysis rate was higher than bacterial N demand only within the deeper layer, and only when considering the high affinity enzyme. Based on a 10% bacterial growth efficiency, the cumulative hydrolysis rates of C-proteins and C-polysaccharides contributed to the heterotrophic bacterial demand, by on average 2.5% ± 1.3 % for the epipelagic layers sampled (sub surface and dcm). This study clearly reveals potential biases in current and past interpretations of the kinetic parameters of the 3 enzymes tested based on their fluorogenic substrates concentration sets. In particular, the aminopeptidase/βglucosidase enzymatic ratios, and some of the depth-related trends, differed between the use of high or low concentrations of the fluorogenic substrates.

1 Introduction

In aquatic environments, the organic matter compounds available for bacterial utilization are dominated by polymeric material (Simon et al., 2002; Aluwihare et al., 1997). In order to be assimilated, first they need to be hydrolyzed into smaller molecules by ectoenzymes. This represents a limiting step in organic matter degradation, and in nutrient regeneration (Hoppe, 1983; Chróst, 1991). Whether the ectoenzymatic activity should be considered as limiting the rate of organic matter remineralization is a subject of debate since hydrolysis and consumption of the by-products of hydrolysis are not always coupled (Smith et al., 1992). Bacterial ectoenzymatic hydrolysis is usually determined using fluorogenic substrates (Hoppe, 1983) which, when cleaved

by the ectoenzyme, triggers the release of a fluorescent by-product. The fluorescence increase is monitored over time, thus allowing the determination of the hydrolysis rate. Kinetic experiments are time-consuming and most studies reporting ectoenzymatic activity examined enzyme kinetic patterns using one or two samples. A single presumably saturating substrate concentration is then used to determine the activity of all the samples. Further, Baltar et al. (2009b) cite a table with 17 published studies on ectoenzymatic activity I which 12 used a single substrate concentration, varying from 0.02 to 1000 µM (with a median of 50 µM). Only 5 studies used a range of substrate concentrations to determine the enzyme kinetics. Of these 5 studies the lowest concentration used was 50 nM, (typically the lower concentration in the set is between 1 and 5 µM), while the highest concentration was 1200 µM (range of the higher concentrations in the set 5 - 1200 µM, with a median of 200 µM). Another compilation of data from the Mediterranean Sea (Zaccone and Caruso; 2019) showed that 6 out of 22 studies used a single concentration (assumed to be saturating) with a median of 125 µM for Leucine 7-amido 4-methyl coumarin and 50 µM for Methylumbellyferyl-phosphate. Likewise, the remaining studies assessed enzyme kinetics with a highly variable range of substrate concentrations (lowest concentrations 0.025-200 µM with a median of 0.1 µM, highest concentrations 1- 4000 µM with a median of 20 µM). However, the combination of: i) non-specificity in the enzymes, ii) the heterogeneity of enzymatic systems within single species, iii) the diversity in species present and iv) the range and variability in concentrations of surrounding substrates, will result in multiphasic kinetics (Chróst, 1991; Arnosti, 2011; Sinsabaugh and Shah, 2012 and references therein). Ectoenzymes are produced by a diversity of microorganisms. Their activity depends on a patchy distribution of natural substrates and a variety of natural (potentially unknown) molecules which can be hydrolyzed by the same enzymes that hydrolyze the added fluorochrome, with potentially different affinities. For instance, cell-specific activities and types of activities were shown to be very variable among 44 heterotrophic bacterial strains isolated from the Californian coast and experimental phytoplankton blooms, from attached particles and in the suspended phase (Martinez et al., 1996). Arrieta and Herndl (2001) assessed the diversity of marine bacterial β-glucosidases taken from a natural community, separated using capillary electrophoresis zymography, and showed that they had different Km and Vm. In the water column different kinetic systems were also observed which are generally attributed to attached or free-living bacteria having different affinities for substrates: k-strategists-oligotrophic bacteria (with both low Km and Vm) or r-strategists/copiotrophic bacteria (with both high Km and Vm, Koch, 2001). At depth, the combination of refractory DOM with recent and freshly sinking particles would promote multiphasic kinetic for ectoenzymatic activity. Biphasic kinetic systems have been described in areas where increasing gradients of polymeric material are expected due to the high concentration of particles; e.g. near the bottom and sediments for aminopeptidase (Tholosan et al., 1999), and in a shallow bay for phosphatases (Bogé et al., 2013). Most studies have shown that cell-specific ectoenzymatic activities on aggregates are ~10 fold higher than those of the surrounding assemblages (for example during a decaying bloom, Martinez et al., 1996). Biphasic kinetics were also attributed to free-living bacteria versus attached heterotrophic bacteria, the latter adapted to cope with high substrate concentrations (with both higher Vm and Km; Unanue et al., 1998). Size fractionation is carried out prior to incubation with fluorogenic substrate in order to determine in which size fraction the activity is dominant. However, size fractionation prior to incubation biases ectoenzymatic activities, due to filtration artifacts and the disrupts of trophic relationships between primary producers, heterotrophic bacteria, protozoans and particulate matter. Despite such biases, carbon budgets have shown that the prokaryotes attached to aggregates are a likely source of by-products for free-living prokaryotes (Smith et al., 1992). Measurements in bulk samples enables

different enzymatic kinetics to be determined without disturbing relationships between free/attached prokaryotes and DOM/POM interactions during the incubations.

In the Mediterranean Sea, elemental C/N/P ratios of dissolved nutrients and organic matter are the subject of particular interest to elucidate the impact of P-deficiency on DOC accumulation in surface waters (Thingstad and Rassoulzadegan, 1995; Krom et al., 2004) given that the export of organic carbon in dissolved *vs.* particulate forms is linked to the P-limitation in surface layers (Guyennon et al., 2015). Since the epipelagic layers are P or N-P limited during most of the stratification period, ectoenzymes such as phosphatase and aminopeptidase providing P and N sources from organic matter have been intensively studied as indicators of these limitations (Sala et al., 2001; Van Wambeke et al., 2002). However, the potential bias introduced by multiple kinetics when comparing different types of ectoenzymes and using variable range of substrates is still poorly understood.

In this study, we investigated the Michaelis-Menten kinetics of three series of enzymes targeting proteins, phospho-mono esters and carbohydrates (leucine aminopeptidase, alkaline phosphatase and β-D –glucosidase, respectively) in the Mediterranean Sea. A wide range of substrate concentrations was tested to evaluate potential multiphasic kinetics. Our aim was to evaluate potential biases in the interpretation of past and current enzymatic kinetics based on studies measuring rates with a reduced range of substrate concentration or with the use of too high substrate concentrations. We also studied the links between ectoenzyme activities with the spatial (vertical and horizontal) trends in the quality of the available organic matter. In fact, the distribution of biogeochemical properties below the productive zone is the result of large-scale dynamic transport systems associated with three distinct thermohaline circulation cells (Wust, 1961; Hopkins, 1978; The Mermex Group, 2011 and references therein). These open cells convey fresh and cool waters of Atlantic origin to the upper 150-200 m water layer extending into the eastern part of the Levantine Sea. The return branch is composed of warm, saline waters, the Levantine intermediate waters (LIW), which spreads over the whole Mediterranean Sea at depths of 200-500 m (Kress et al., 2003; Malanotte-Rizzoli et al., 2003; Schroeder et al., 2020). In addition, two closed cells, internal to each Mediterranean sub-basin, are driven by deep water convection and spread below the LIW (e.g., Lascaratos et al., 1999; Testor et al., 2018).

This study focuses on the open waters of the Mediterranean Sea, examining four water layers: surface (generally P or N limited in stratification period), the deep chlorophyll maximum layer (coinciding with nutricline depths), the LIW and the deep waters. Alongside marine biogeochemical fluxes, atmospheric fluxes were quantified simultaneously during the same cruise. As a result of these exceptional simultaneous measurements of fluxes on the same cruise, the data used in this manuscript are also used in another article of this special issue (Van Wambeke et al., 2020) where biogeochemical fluxes within the mixed layers are compared to wet and dry N and P atmospheric fluxes.

2. Materials and Methods

2.1 Sampling strategy

The PEACETIME cruise (doi.org/10.17600/15000900) was conducted from May to June 2017, along a transect extending from the Western Mediterranean Basin to the center of the Ionian Sea (25°S 115 E – 15°S, 149°W, Fig. 1). For details on the cruise strategy, see Guieu et al. (2020). Stations of short duration (< 8 h, 15 stations named SD1 to SD10, Fig. 1) and long duration (5 days,

3 stations named TYR, ION and FAST) were sampled. Generally, at least 3 casts were conducted at each short station. One focused on the first 250 m and the second one on the whole water column. These 2 casts were sampled with a standard, CTD rosette equipped with 24 Niskin bottles (12 L), and a Sea-Bird SBE9 underwater unit equipped with pressure, temperature (SBE3), conductivity (SBE4), chlorophyll fluorescence (Chelsea Acquatracka) and oxygen (SBE43) sensors. The third cast (from surface to bottom) was carried out using a trace metal clean (TMC) rosette mounted on a Kevlar cable and equipped with Go-Flo bottles that were sampled in a dedicated trace metal free-container. The long stations situated in the center of the Tyrrhenian Sea (TYR), in the center of the Ionian Sea (ION) and in the western Algerian Basin (FAST) were selected using satellite imagery, altimetry and Lagrangian diagnostics to target dust deposition events (Guieu et al., 2020). At these stations, repeated casts were performed, alternating CTD- and TMC- rosettes.

The water sampled with the conventional CTD-rosette was used for measurements of heterotrophic bacterial production (BP, *sensus stricto* referring to heterotrophic prokaryotic production), heterotrophic bacterial abundances (BA, *sensus stricto* referring to heterotrophic prokaryotic abundances), ectoenzymatic activities (EEA), chlorophyll stocks, particulate organic carbon (POC), nitrogen (PON), phosphorus (POP) and dissolved organic carbon (DOC). Dissolved inorganic nitrogen (DIN) and phosphorus (DIP), dissolved organic nitrogen (DON) and phosphorus (DOP) were collected using the TMC-rosette

Details on the sampling and analysis for the additional parameters data presented in this paper (hydrographic properties, total chlorophyll a (Tchl-a) are available in Taillandier et al. (2020), Guieu et al. (2020), and Marañón et al. (2020), in this issue.

We focused on 4 layers of the water column: two in epipelagic waters: at 5 m near the surface (SURF) and in the deep chlorophyll maximum layer (DCM) localized by the *in vivo* fluorescence measured continuously during downcasts, and two in deeper layers: in the LIW localized by sub-surface salinity maximum and oxygen minimum during downcasts (named LIW), and at 1000 m (the limit between meso and bathypelagic waters, named MDW), except at 2 stations : FAST, 2500 m and ION, 3000 m (Table 1).

2.2 Biochemistry

Nitrate (abbreviated as NO3), nitrite (NO2), and orthophosphate (DIP) concentrations were determined using a segmented flow auto-analyzer (AAIII HR Seal Analytical) according to Aminot and Kérouel (2007). The detection limits were 0.05 µM for NO3, 0.01 µM for NO2 and 0.02 µM for DIP. DON and DOP were determined after high-temperature (120 °C) persulfate wet oxidation mineralization (Raimbault et al., 1999) as follows: water sample was filtered through a 0.2 µm PES membrane and collected into 25 ml glass flasks. Samples were immediately poisoned with 100 µl H_2SO_4 5N and stored in the dark until analysis in the laboratory. Filtered samples (20 mL) were then transferred in Teflon vials for wet oxidation. Nitrate and phosphate formed corresponding to the total N and P in the dissolved pool (TDN and TDP) and were determined as described for dissolved inorganic nutrients. DON and DOP were obtained from the difference between TDN and DIN, and TDP and DIP, respectively. The limits of detection were 0.5 and 0.02 µM for DON and DOP, respectively.

Particulate organic nitrogen and phosphate (PON, POP) were determined using the same wet oxidation method (Raimbault et al., 1999). Samples (1.2 L) were collected into polycarbonate bottles and filtered through pre-combusted (450 °C, 4 h) glass fiber filters (Whatman 47mm GF/F).

Filters were storen at -20°C until analysis in the laboratory, where they were placed in Teflon vials with 20 mL of ultrapure water (Milli-Q grade) and 2.5 mL of the wet oxidation reagent for mineralization. The nitrate and orthophosphate produced were analyzed as described previously. The limits of quantification were 0.02 and 0.001 μM for PON and POP, respectively.

In the epipelagic samples from nutrient-depleted layers, DIP and NO3 were determined using the liquid waveguide capillary cell method (LWCC) (Zhang and Chi, 2002) whereby the sensitivity of the spectrophotometric measurement was improved by increasing the length of the optical path of the measurement cell to 2.5 m. For DIP, detection limits lowered to 0.8 nM and the response was linear up to about 150 nM, for NO3, detection limits lowered to 9 nM.

Samples for dissolved organic carbon (DOC) were filtered through two pre-combusted (24 h, 450°C) glass fiber filters (Whatman GF/F, 25 mm) using a custom-made glass/Teflon filtration syringe system. Samples (10 mL in duplicates) were collected into pre-combusted glass ampoules and acidified to pH 2 with phosphoric acid (H_3PO_4). Ampoules were immediately sealed and storen in the dark at room temperature .Samples were analyzed by high temperature catalytic oxidation (HTCO) on a Shimadzu TOC-V-CSH analyzer (Cauwet, 1999). Prior to injection, DOC samples were sparged with CO_2 -free air for 6 min to remove inorganic carbon. 100 μL of samples were injected in triplicate and the analytical precision was 2%. Consensus reference materials (http://www.rsmas.miami.edu/groups/biogeochem/CRM.html) were injected every 12 to 17 samples to insure stable operating conditions. The nominal and measured DOC concentrations of the two batches used in this study were 42-45 μM and 43-45 μM, respectively, for batch14-2014#07-14, and 42-45 μM and 42-49 μM, respectively, for batch17-2017 #04-17. Particulate organic carbon (POC) was measured using a CHN analyzer using the improved analysis proposed by Sharp (1974).

Samples (20 ml) for total hydrolysable carbohydrates (TCHO) > 1 kDa were collected into precombusted glass vials (8 h at 500°C) and stored at -20°C until analysis. Samples were desalinated using membrane dialysis (1 kDa MWCO, Spectra Por) at 1°C for 5 h. Samples were then hydrolyzed for 20 h at 100°C with 0.8 M HCl final concentration with subsequent neutralization using acid evaporation (N_2, for 5 h at 50°C). TCHO was analyzed using high performance anion exchange chromatography with pulsed amperometric detection (HPAEC-PAD) which was applied on a Dionex ICS 3000 ion chromatography system (Engel and Händel, 2011). Two replicates for each TCHO sample were analyzed.

Total hydrolysable amino acids (TAA) were determined from 5 mL water sample collected into precombusted glass vials (8 h, 500°C) and stored at -20°C. Samples were measured in duplicates. The samples were hydrolyzed at 100°C for 20 h with 1 mL 30% HCl (Suprapur®, Merck) per 1 mL of sample and neutralized by acid evaporation under vacuum at 60°C in a microwave. Samples were analyzed using high performance liquid chromatography (HPLC) on an Agilent 1260 HPLC system following a modified version of established methods (Lindroth and Mopper, 1979; Dittmar et al., 2009). Prior to the separation of 13 amino acids with a C^{18} column (Phenomenex Kinetex, 2.6 μm, 150 x 4.6 mm), in-line derivatization with o-phthaldialdehyde and mercaptoethanol was carried out. A gradient with solvent A containing 5 % acetonitrile (LiChrosolv, Merck, HPLC gradient grade) in sodiumdihydrogenphosphate (Suprapur®, Merck) buffer (pH 7.0) and acetonitrile as solvent B was used for analysis. A gradient from 100 % solvent A to 78 % solvent A was produced in 50 min.

2.3 Bacterial production

BP was determined onboard using the ^{3}H- leucine (^{3}H-Leu) incorporation technique (Smith and Azam, 1992) and the microcentrifuge method for epipelagic water samples, and the filtration technique for deep water samples; the centrifuge technique is limited to incubation volumes of 1.5 mL and not sensitive for deep water communities. For SURF and DCM layers, triplicate 1.5 mL samples and a control killed with trichloracetic acid (TCA, 5 % final concentration) were incubated with a mixture of [4,5-^{3}H]-leucine (Amersham, specific activity 112 Ci mmol^{-1}) and nonradioactive leucine at final concentrations of 7 and 13 nM, respectively. Samples were incubated in the dark at the respective *in situ* temperatures for 1- 4 h. On 9 occasions during the cruise transect, we checked that the incorporation of leucine was linear with time. Incubations were ended by the addition of TCA to a final concentration of 5 %, followed by three runs of centrifugation at 16000 g for 10 minutes. Bovine serum albumin (BSA, Sigma, 100 mg L^{-1} final concentration) was added before the first centrifugation. After discarding the supernatant, 1.5 mL of 5 % TCA was added before the second centrifugation, and after discarding the supernatant, 1.5 mL of 80 % ethanol was added. After the third centrifugation,the ethanol supernatant was then discarded and 1.5 mL of liquid scintillation cocktail (Packard Ultimagold MV) was added. For the LIW and MDW layers, 40 mL samples were incubated in the dark for up to 12 hours at *in situ* temperature (triplicate live samples and one control fixed with 2% formalin), with 10 nM [4,5-^{3}H]-leucine. After filtration of the sample through 0.2 µm polycarbonate filters, 5% final concentration TCA was added for 10 minutes, subsequently then the filter was rinsed with 10 mL 5% TCA and a final rinse with 80% ethanol.

For both types of samples (centrifuge tubes and filters) the incorporated radioactivity was counted using a Packard LS 1600 Liquid Scintillation Counter on board the ship. A factor of 1.5 kg C mol leucine^{-1} was used to convert leucine incorporation to carbon, assuming no isotopic dilution (Kirchman, 1993), as checked using occasional concentration kinetics. Standard deviations from triplicate measurements averaged 8 % and 25 % for BP values estimated with the centrifugation (surface layers) or the filtration technique (deep layers), respectively.

2.4 Ectoenzymatic activities

EEA were measured fluorometrically, using the following fluorogenic model substrates: L-leucine-7-amido-4-methyl-coumarin (Leu-MCA), 4 methylumbelliferyl – phosphate (MUF-P), 4 methylumbelliferyl – βD-glucopyranoside (MUF-βglu) to track aminopeptidase activity (LAP), alkaline phosphatase activity (AP), and β−glucosidase activity (βGLU), respectively (Hoppe, 1983). Stock solutions (5 mM) were prepared in methycellosolve and stored at −20°C. The amounts of MCA and MUF products released by LAP, AP and βGLU activities after addition of substrate concentrations ranging from 0.025 to 50 µM, were followed by measuring the increase in fluorescence (exc/em 380/440 nm for MCA and 365/450 nm for MUF, wavelength width 5 nm) in a VARIOSCAN LUX microplate reader. The instrument was calibrated with standards of MCA and MUF solutions diluted in filtered (< 0.2 µm) boiled seawater. For measurements, 2 mL of unfiltered seawater samples were supplemented with 100 µL of a fluorogenic substrate solution in a black 24-well polystyrene plate in duplicate. Three plates were filled per layer and analyzed with the different substrates MUF-P, MCA-leu and MUF-βglu. Incubations were carried out in the dark in thermostatically controlled incubators at *in situ* temperatures. Incubations lasted up to 24 h, with fluorescence measurements every 1 to 3 h, depending on the expected activities. The enzyme hydrolysis rate (V) was calculated from the linear part of the fluorescence versus time relationship. Boiled-water blanks were run to check for abiotic activity. The parameters Vm (maximum hydrolysis velocity) and Km (Michaelis-Menten half-saturation constant which reflects enzyme

affinity for the substrate) were estimated by non-linear regression of the Michaelis-Menten function : V = Vm × S/(Km + S), to the hydrolysis rate (V) as a function of the fluorogenic substrate concentration (S) using PRISM4 (Graph Pad software, San Diego, USA) We determined Vm and Km using 3 series of substrate concentrations: Vm_{all} and Km_{all} (global model) were calculated using a range of 11 concentrations (0.025, 0.05, 0.1, 0.25, 0.5, 1, 2.5, 5, 10, 25 and 50 µM) in duplicate, Vm_1 and Km_1 (model 1) were calculated using a restricted substrate concentration set up to 1 µM (0.025, 0.05, 0.1, 0.25, 0.5, 1 µM) in duplicate, and Vm_{50} and Km_{50} (model 50) were calculated using the concentration set restricted to the high values of substrate (2.5, 5, 10, 25, 50 µM). We used the term 'ectoenzyme' for all types of enzymes found outside the cell, including enzymes attached on external membranes, or within the periplasmic space), or free-dissolved enzymes, to broadly encompasses all enzymes located outside of intact cells regardless of the process by which such enzymes entered the environment.

We used an approach similar to Hoppe et al. (1993) to compute *in situ* hydrolysis rates for LAP and βGLU (the calculation for AP is presented in a companion paper from this issue by Pulido-Villena et al., in prep), using total carbohydrates (TCHO) and total aminoacids (TAA) concentrations in water samples as representative of dissolved carbohydrates and proteins, respectively. These rates were calculated based on Vm_1 and Km_1, on one hand and on Vm_{all} and Km_{all}, for the other. *In situ* hydrolysis rates expressed in nmol substrate L^{-1} h^{-1} were then converted into carbon and nitrogen units using C/TCHO, C/TAA and N/TAA molar ratios.

2.5 Statistics

To assess biphasic trends within ectoenzymatic activities, firstly, we rejected all kinetics where the coefficient of variation (standard error/mean ratio) of Vm or Km was greater than 100%. For the remaining kinetics, secondly, we used the F-test of Fisher-Snedecor as developed in Tholosan et al. (1999) to ascertain whether 2 additional parameters (Vm_1, km_1 and $Vm_{50,}$ Km_{50} instead of Vm_{all} and Km_{all}) improved the model significantly based on the following series of equations:

$$\text{Cost (Vm, Km)} = \text{sigma } [(\text{Vdata-Vfit})/w]^2$$

where Vdata is the experimental hydrolysis rate, Vfit the corresponding value of the fitted function, w a weighting factor set to 1, like assumed in Tholosan et al (1999). The cost function was determined for the global model fitted with the entire set of concentrations ($cost_{all}$), the model 1 with low concentrations ($cost_1$), and the model 50 with large concentrations ($cost_{50}$) as:

$$\text{Var (additional parameters)} = (cost_{all} - cost_1 - cost_{50}) / 2$$

$$\text{Var (biphasic)} = (cost_1 + cost_{50}) / (n - 4)$$

Where n is the number of concentrations data in the entire data set. These 2 variances where finally compared using the F test:

$$F_{(2,\ n-4)} = \text{var (additional parameters)/var (biphasic)}$$

When the F test showed that the variances were significantly different at a probability of 0.1 we assumed that the biphasic mode was meaningful enough to explain the kinetics of the entire data set.

Trends with depth were estimated using a depth variation factor (DVF) estimated as the mean of pooled SURF and DCM data divided by the mean of pooled LIW and MDW data. This decrease (or

increase), was considered as significant after a t-test comparing both series of data. The type of t test used depended on the result of a preliminary F-test checking for variance. Coefficient of variation (CV) was calculated as: standard deviation/mean x 100. Correlations among variables were examined after log transformation of the data. All mean of 'ratios' cited in the text (Vm_{all}/Vm_1, Km_{all}/Km_1, DVF, Km/Vm, DOC/DOP, DOC/DON, TAA/DON, TCHO/DOC… are computed from means of ratios and not from the ratio of means.

3. Results

3.1 Physical properties

The physical properties at the sampled stations (Fig. 2), show pronounced longitudinal variation which is in agreement with the thermohaline circulation features of the Mediterranean Sea (see Introduction). The deep waters, formed by two separate internal convection cells, have distinct properties in the Eastern basin (station ION, temperature 13.43°C, salinity 38.73) and the Western basin (the other stations, temperature 12.91°C, salinity 38.48). The deep layer samples MDW were collected within or in the top of deep waters (grey dots, Fig. 2). The intermediate layer samples LIW were collected in the vicinity of the salinity maxima (red dots, Fig.2), which is used to identify the LIW cores (e.g., Wust, 1961). Salinity maxima in the LIW core are particularly pronounced in the presence of fresher and lighter waters of Atlantic origin above, this feature is progressively relaxed eastward. LIW properties decrease from ION, the closest station from their source, to the westernmost stations of the Algerian Basin, which is concurrent with their westward spreading and progressive dilution. In this springtime period, the productive layer was stratified with the apparition of a seasonal thermocline. This interface separated the warm surface waters with the cool waters of Atlantic origin in which the DCM developed. As a consequence the two sample types collected in the productive layer (SURF in blue dots and DCM in green dots, Fig. 2), have their thermohaline properties similar in salinity, but clearly differentiated in temperature. For sake of clarity, the stations are ranked with respect to these longitudinal variations, in the following order: ST10, FAST, ST1, ST2, ST3, ST4, ST5, TYR, ST6 and ION.

3.2 Biogeochemical properties

Nitrate and phosphate were depleted in the surface layers, with concentrations below the detection limits of classical methods (0.01 µM, Table S1). Using the LWCC technique, however, DIP could be detected (Table S1) and ranged between 4 to 17 nM at 5 m depth (Table S1). Phosphaclines were deeper than nitraclines and deeper in the Eastern basin, particularly at ST 6 and ION. Chlorophyll standing stocks ranged from 18.7 to 35 mg Tchl*a* m^{-2} at ST 6 and ST1, respectively (Table 1). The depth of the DCM ranged from 49 to 83 m depth in the Western basin, exhibiting the deepest value in the Ionian Sea (105 m depth at ION) while no obvious trend has been observed in the Tyrrhenian Sea.

DOC ranged from 39 to 75 µM (Table S1). Highest DOC values were generally observed in the surface layers and decreased by approximately 10 µM in each consecutive layer sampled. The DOC depth variation factor ranged from x1.2 to x1.6. DON ranged from 2.5 to 10.4 µM. The DON depth variation factor (DVF) was close to that of DOC (x1.2 to x1.8). DOP ranged from detection limits to 0.09 µM. Taking all the 4 water layers, the mean value for the DOC/DON and DOC/DOP molar ratios were 14 ± 2 and 2112 ± 1644, respectively with no significant change of these ratios between SURF and DCM layers compared to LIW and MDW layers due to the variability between stations. Deep DOP was not sampled at 3 stations. DOP estimate is subject to large errors at depth (DIP is on

average 10 times higher than DOP). We observed a DOC/DOP increase at the 2 deep layers sampled at 4 stations, a decrease at 2, and no trend at another.

The mean values of TAA were stable between SURF and DCM layers, around 210 nM (Table S1, Fig. S1a). At all stations TAA decreased from the 2 layers sampled in the epipelagic layers compared to the 2 other deeper layers (LIW and MDW) sampled ($p < 0.001$). The mean DVF of TAA (x3.4) was twice as high as that of DON (x1.5) and as a consequence TAA-N to DON ratio (Fig. S1a) decreased significantly ($p < 0.001$) in the 2 deep layers compared to the 2 epipelagic layers (Fig S1a). TCHO ranged from 111 to 950 nM and the contribution of TCHO-C to DOC from 1.3 to 9.7% (Fig. S1b). At 6 stations out of 10, a minimum TCHO value was obtained within the LIW layer (Fig. S1b). The TCHO-C to TAA-C ratio increased significantly at the 2 deep layers compared to the 2 epipelagic layers ($p < 0.02$) and exhibited particularly high ratios within the Tyrrhenian sea MDW layer (ST5: 48, TYR: 24, ST6: 27).

3.3 Ectoenzymatic activities – kinetic trends

Different types of kinetics were obtained (see examples in Fig. 3). In general, the hydrolysis of LAP and βGLU did not completely saturate at the substrate concentration of 50 µM but started to reach the asymptotic value of Vm and the hydrolysis rate of AP stabilized around 1 µM MUF-P. In this example, significant fits to Michaelis-Menten kinetic were obtained using either the model 1, the model 50 or the global model. However, significant Michaelis-Menten kinetics were also obtained regardless of the highest pair of values (concentration, rate) included in the fit (Fig. S2 a, b, c). The Vm and Km characterizing these kinetics increased according the highest concentration included in the model, but tended to reach a plateau (more rapidly for AP, Fig. S2 c and f). In order to check the presence of biphasic kinetic, and to focus on the effect of choosing the two extreme sets of concentrations ranges, EEA kinetic parameters were then systematically determined using the model 50 (Vm_{50}, Km_{50}), the model 1 (Km_1, Vm_1) or the global model (Km_{all}, Vm_{all}). Our choice to use model 1 corresponds to a compromise between sufficient substrate concentrations in the lowest range with significant rates detected. Some kinetics were discarded i) due to the limit of detection of some rates, particularly at low concentration of substrates (it was the case for all the βGLU estimates in LIW and MDW layers, Table S2), ii) due to a significant deviation from the model (in particular, when the rates were not increasing between 2.5 and 50 µM addition of substrate, leading to abnormally low values of Km_{50}. This was noted in particular for AP as only 25 kinetics over 40 of the model based on high concentrations of substrates were significant (see AP model 50, Table S2).

For LAP and βGLU, Vm_{all} and Vm_{50} were close, the distribution of these data fitted to the 1:1 axis (Fig. 4). Note however that the standard error of Vm_{50} were higher than those of their corresponding Vm_{all} (Fig. 4, Table S2). The relationships between Km_{50} and Km_{all} showed the same trend, although Km_{50} were generally slightly higher than their corresponding Km_{all}, in particular for βGLU. The standard errors of Km were higher than those of their corresponding Vm (Table S2). For LAP and βGLU, Vm_1 was notably lower than Vm_{50} and Vm_{all}; Km_1 was notably lower than Km_{50} and Km_{all}. For AP, the difference between Vm_1 and Vm_{50} was not such evident, Vm_1 being closer to Vm_{50}. However, Km_{50} was generally still much higher than Km_1.

The biphasic mode itself explained the kinetics of the entire data set in 17 cases out of 40 for LAP, in 18 cases out of 20 for βGLU and in18 cases out of 24 for AP (Table S2). Thus, the biphasic mode was enough on average to explain 60 % of the cases, and in the greatest proportions for

βGLU. We estimated the degree of difference between the two kinetics using the 'biphasic indicator' developed in Tholosan et al. (1999). This index tracks the difference between the initial slopes (Vm/Km) of Michaelis-Menten kinetics as (Vm_1/Km_1) / (Vm_{50}/Km_{50}). The biphasic indicator was particularly marked for βGLU (means of 68 in SURF and 29 in DCM layers), but it was highly variable (range 5 - 153). For LAP the mean index increased significantly ($p < 0.01$) from about ~4 in SURF and DCM layers (range 1 - 10) to 14 and 24 within LIW and MDW layers (range 2 - 86), respectively. For AP the index remained constant ($p > 0.05$) between epipelagic layers (means 2.8, 1.9 in SURF and DCM) and deeper layers sampled (means of 2.4 and 3.2 in LIW and MDW, respectively).

As the constants Km and Vm provided by the global model were very close to those of the model 50, as the standard errors were systematically higher using the model 50 compared to the global model and because the biphasic mode was not systematic, we present below only vertical and longitudinal distribution of the kinetic parameters for the global model and for the model 1 (Figs. 5, 6, 7 and Table 2). Moreover, as already mentioned, the aim of this paper was not to discuss strictly on biphasic kinetics but to highlight the importance of choosing appropriate concentration range in substrates. The lowest concentration range represents the more realistic estimation considering the natural substrate concentrations. This will allow do discuss then the biases introduced by choosing a low (0.025-1 µM) set of concentration compared to a set reaching much higher concentration (here up to 50 µM) generally used by scientists making enzymatic kinetics (see the first part of the discussion).

For each enzyme (LAP, βGLU, AP) and each model (model 1 or global model), the order of magnitude reached for Vm was the same at the SURF and DCM layers (Figs 4, 5, 6). In all layers, the highest mean Vm of the 10 studied stations was obtained for AP, followed by LAP and then βGLU, whatever the range of tested concentrations (Vm_{all} or Vm_1, Table 2).

For LAP (Fig. 5), Vm_{all} was on average 3 times higher than Vm_1 in both SURF and DCM layers, but the differences between these two rates increased with depth (x8 in LIW, x12 in MDW layers). Vm_{all} decreased from epipelagic to mesopelagic layers by a factor DVF of x8 on average, while Vm_1 decreased by a factor x19 (Fig. 5a). However, if this decrease was particularly obvious for both for Vm_1 and Vm_{all} at stations ST10 to ST5 in the Western Basin, it was not the case for Tyrrhenian waters (ST5, TYR and ST6) where Vm_1 decreased with depth but not as much Vm_{all}. The average Km_{all}/Km_1 ratio for LAP was 132. Km_{all} of LAP showed variable patterns with depth. Within LIW layers, Km_{all} were in the same order of magnitude as in the surface, sometimes even higher (FAST, ST 3, ST5, ST6, ION) as well as in the MDW layers particularly in Tyrrhenian and Ionian seas (Fig. 5b). On the other hand, Km_1 decreased with depth in the Western stations (ST10 to ST3) whereas for stations 4, 6 and ION the order of magnitude of Km_1 at all depths were similar.

For the LIW and MDW layers computation of βGLU kinetic was impossible as as the linearity of fluorescence versus time was observed only for the higher concentrations used. The means of βGLU rates measurable at depth were 0.010 ± 0.006 nmol L^{-1} h^{-1} in the LIW layer and 0.008 ± 0.006 nmol L^{-1} h^{-1} in the MDW layer (Fig. 6, Table 2). In the epipelagic layers (Fig. 6), Vm_{all} was on average 7 and 5 times higher than Vm_1 in SURF and DCM layers, respectively. The ratio Vm_{all}/Vm_1 was greater than those observed at the same layers for LAP or AP (Fig. 6a). The average Km_{all}/Km_1 ratio for βGLU was 311. While Km_{all} was of the same order of magnitude or slightly lower within the DCM layers compared to the SURF layers, the opposite trend was observed for Km_1 which tended to be equal or higher within the DCM layer (Fig. 6b). Among the 3 ectoenzymes,

βGLU showed the lowest longitudinal variability within surface layers (the longitudinal CV was 34% for Vm_{all}, 45% for Vm_1, Table 2).

AP was the enzyme for which Vm_1 and Vm_{all} were the closest (average of Vm_{all} /Vm_1 ratio for the whole data set was 1.9 ± 1.2) (Fig. 7a), confirming that saturation rates occurred with 1 µM MUF-P addition (Figs. 3, S2) and explained why fits to model 50, using 2.5 to 50 µM concentration sets, were often not significant (Table S2). AP within SURF layer showed a larger range of longitudinal variability than the remaining studied ectoenzymes, with longitudinal CV close to 100% for Vm_{all} and Vm_1 (Table 2). The trend within SURF layers was an increase of AP towards the east, from a range of 0.5-0.9 nmol L^{-1} h^{-1} for Vm_{all} at ST10 and FAST and up to 8 nmol L^{-1} h^{-1} at ION. Both AP Vm_1 and Vm_{all} decreased with depth (Fig. 7a), although sometimes both AP Vm_{all} and AP Vm_1 within the DCM layer were higher than within the surface (ST1, 2, 5 TYR, ION). At all stations Vm in MDW were equal or lower to those within LIW layers. DVF was large, varying from x1.8 to x71 for Vm_{all}, with lower decreases with depths at ST10 (x1.8) FAST (x3.2) and ST3 (x 2.4), and highest DVF at ST1 (x34), ST2 (x71) and ION (x54). While Vm_1 and Vm_{all} were almost equal, AP Km_{all} was on average 6 times higher than Km_1.It was observed that the general trend was that Km_{all} increased more with depth (DVF > 0 at 8 stations and ranging from x1.4 to x19) than Km_1 (DVF > 0 at 9 stations and ranging x1.9 to x3.8, see ST1 and ST5). However, these differences between AP Km_1 and AP Km_{all} were still the lowest compared to the two other enzymes.

The turnover time of ectoenzymes was determined as the Km/Vm ratio, which drives the activity at low concentrations of substrates. The incidence of the tested set of substrate concentration is very important on this parameter, as turnover times are systematically lower for the 0.025-1 µM concentration set (Table 3). The turnover times were the shortest for AP and the longest for βGLU.

3.4 Specific activities

Both BP and BA were used to compute specific activities (Table 2, Fig S3). Bulk heterotrophic prokaryotic production (BP) was of the same order of magnitude within SURF and DCM layers and decreased within LIW and MDW layers (DVF 59 ± 23). Per layer, BA were less variable than EEAs or BP. BA decreased with depth less rapidly than BP (DVF 7 ± 2). Specific BP ranged from 1 to 136 x 10^{-18} g C $cell^{-1}$ h^{-1} (Table 4), exhibiting a decrease with depth at all stations (DVF ranged x4 - x23). For EEAs (AP, LAP, βGLU) and BP, the trend of specific activities with depth was highly variable among the different stations (Fig. 8), with the highest DVF (decrease with depth) observed for BP per cell or AP per cell.

For LAP, specific activities per bacterial cell ranged from 0.1 - 2.1 x 10^{-18} to 0.7 - 8 x 10^{-18} mol leu $cell^{-1}$ h^{-1}, based on Vm_1 and Vm_{all} rates, respectively (Fig. 8 a, b; Table 4 for Vm_1). A significant decrease with depth from epipelagic waters to deep waters was obtained only for cell-specific Vm_1 LAP, but not for cell-specific Vm_{all} LAP ($p < 0.001$). While the specific LAP Vm_1 per unit cell decreased with depth, the LAP Vm_1 per unit BP increased with depth at all stations (Table 4, Fig. 9a).

For AP, per cell-specific activities ranged from 0.11 to 32 x 10^{-18} mol P $cell^{-1}$ $h^{-1}$and from 0.14 to 39 x 10^{-18} mol P $cell^{-1}$ h^{-1} based on Vm_1 and Vm_{all} rates, respectively, not differing significantly due to the small differences between AP Vm_1 and AP Vm_{all} (Fig. 8 c, d). Cell-specific AP exhibited either an increase (DVF < 1) or a decrease (DVF >1) with depth (Fig. 9b). AP Vm_1 per unit BP decreased with depth at all stations except at ION, whereas AP Vm_1 per unit cell increased in 7 cases over 10 .

3.5 In situ hydrolysis rates

The *in situ* hydrolysis rates of TAA by LAP were higher using Vm_1 and Km_1 constants than using Km_{all} and Vm_{all}, about ~3 times in epipelagic and about ~7 times in deep waters (Fig. 10). Km_{all} were much higher than TAA concentrations (means ranged 26 to 300-fold according layers, Table 2, Table S1). This difference was still visible but highly lowered considering Km_1, as ratio between Km_1 and TAA differed by factor of 2 to 3 according to the layer considered. Consequently, *in situ* TAA hydrolysis rates by LAP based on Km_{all} and Vm_{all} represented a small percentage of Vm_{all} (maximal means per layer were 11 % in the DCM layer and minimal 0.6 % in the MDW layer). However, based on Km_1 and Vm_1, *in situ* rates were relatively higher but in constant proportion relative to Vm_1 (means 30 to 39 % depending on the layer).

The *in situ* hydrolysis rates of TCHO by βGLU were higher using Vm_1 and Km_1 constants than using Km_{all} and Vm_{all}, by ~2.5 times in epipelagic layers (Fig. 11). Km_{all} were higher than TCHO concentrations (Table 2, Table S1), about ~ 18 times within SURF and 22 times within DCM layers. Consequently, *in situ* βGLU hydrolysis rates based on Km_{all} and Vm_{all} were quasi proportional to the turnover rate $Vm_1/Km_1$and represented a mean of 7% of the Vm_{all} in epipelagic layers. At the opposite, Km_1 were much lower than TCHO concentrations (about ~ 31 times in SURF, 8 times at the DCM) and thus most *in situ* rates based on Km_1 and Vm_1 were close to Vm_1 (93% in SURF, 79% at the DCM).

4. Discussion

4.1 The use of a broader set of substrate concentrations changes our interpretation of ectoenzymes kinetics

The idea that ectoenzyme kinetics are not monophasic is neither new nor surprising (Sinsabaugh and Shah, 2012 and references therein). However, despite the 'sea of gradients' encountered by marine bacteria (Stocker, 2012), multiphasic kinetics are seldomly considered. In this work, we attempt to compare different concentration sets of fluorogenic substrates in order to evaluate the consequences on the estimated kinetic parameters in relation to the *in situ* natural concentrations of the substrates. In the coastal, epipelagic waters of the Mediterranean Sea, Unanue et al. (1999) used a set of concentrations ranging from 1 nM to 500 µM to reveal biphasic kinetics with a switch between the two phases at around 10 µM for LAP and 1-25 µM for βGLU. They referred to 'low affinity' enzymes' and 'high affinity' enzymes. In the Toulon Bay (NW Mediterranean Sea), Bogé et al. (2012) used a MUF-P range from 0.03 to 30 µM and described biphasic AP kinetics, with a switch between the 2 enzymatic systems around 0.4 µM. In our study, the biphastic indicator $(Km_{50}/Vm_{50}) / (Km_1/Vm_1)$ was used to determine the degree of difference between the two Michaelis-Menten LAP kinetics and this indicator increased with depth. The two LAP enzymatic systems observed in the water column could reach a difference as large as that found in sediment (about 20, Tholosan et al., 1999), in which large gradients of organic matter concentrations are found. However, this was not the case for all enzymes: for AP, the differences were small and relatively consistent with depth. Finally, the differences between the high and low affinity enzyme was greater for βGLU.

By comparing model 1, model 50 and the global model, and from the analysis presented in Fig S2, it is clear that the choice of the highest concentration used in the Michaelis-Menten kinetic is crucial. We decided thus not to focus our discussion on the presence or not of biphasic kinetics.

Rather, we compared the effects of choosing a set of concentrations ranges sufficiently low to obtain measurable rates but at the same time encompassing the natural range of substrates (the high affinity system). We discuss the enzymatic properties obtained to the global model which, setting the higher concentration to 50 µM reflects better the concentration generally used in the literature and. In addition the comparison between kinetic parameters from model 1 and model 50 shows that it reflected a low affinity system compared to model 1.

Ratios of enzymatic kinetic parameters are also relevant information for the interpretation of the hydrolysis of the substrate in terms of quality and quantity. For instance, the LAP Km_{all} is largely higher than βGLU Km_{all} probably because LAP is not adapted to face low concentration ranges, in contrast to βGLU (Christian and Karl, 1995). It is also possible, however, that when the fluorogenic substrates have the same concentration range as the natural substrates used by the enzyme of interest, this leads to a competition for the active sites. We thus assumed that Km_1, although lower than published values, are still potentially overestimated. Another difference in the response to the tested range of concentrations for each substrate was the turnover time (Km/Vm ratio): the lower the Km/Vm, the better the adaptation to hydrolyze substrates at low concentrations. This should be considered carefully when comparing reported values.

We have shown that the differences between the Km and Vm of the low and high affinity enzymes might change with the nature of the enzyme, with depth, and regionally. We will develop the different interpretation emerging from i) the increase/decrease with depth ii) the use of enzymatic ratio as indicators of nutrient availability or DOM quality and iii) the estimates of *in situ* hydrolysis rates and their contribution to heterotrophic bacterial carbon or nitrogen demand.

4.2 How the set of concentration used affects ectoenzymatic kinetic trends with depth: possible links with access to particles

We have shown that, depending on the range of concentrations tested, different conclusions can be drawn regarding the debate on increasing or at least maintenance of specific levels of activity within deep layers (Koike and Nagata, 1997; Hoppe and Ulrich, 1999; Baltar et al., 2009b). Many factors, such as the freshness of the suspended particles, particle fluxes, a recent convection event, lateral advection from the margins, as well as the seasonality and taxonomic composition of phytoplankton could influence dynamics at depth, particularly in the mesopelagic layers (Tamburini et al. 2002; 2009; Azzaro et al., 2012; Caruso et al 2013; Severin et al. 2016).

AP was the enzyme that showed the smallest contrasts between both kinetics. In this study, the use of MUF-P concentrations ranging between 0.025 and 50 µM highlighted that AP rates fit well with the Michaelis-Menten Kinetic model, with saturation reached at 1 µM. We thus assumed that this AP activity should belong to free-living bacteria and/or dissolved enzymes (< 0.2 µm fraction) with affinities adapted to low substrate concentrations. These results agree with average DOP concentrations measured, ranging between 12 and 122 nM in epipelagic waters (Pulido-Villena et al., this issue in prep) and, when detectable, ~ 40 nM in deep layers. Using fractionation-filtration procedures, it has been shown that more than 50 % of the AP activity could be measured in the < 0.2 µm size fraction (Baltar, 2018 and references therein), whereas the dissolved fraction of other enzymes is generally lower. Hoppe and Ulrich (1999) found a contribution of the < 0.2 µm fraction of 41% for AP, 22 % for LAP and only 10 % for βGLU. During the PEACETIME cruise we ran some size fractionation experiments in SURF and DCM layers (results not shown). The contribution

of the < 0.2 µm fraction to the bulk activity was on average 60 ± 34 % (n = 12) for AP, 25 ± 16 % (n = 12) for βGLU and 41 ± 16 % (n = 12) for LAP, confirming these trends in the Mediterranean Sea.

Increasing AP activities per cell with depth has been reported in the Indian Ocean (down to 3000 m-depth; Hoppe and Ullrich,1999), in the subtropical Atlantic Ocean (down to 4500 m-depth; Baltar et al.; 2009b) and in the central Pacific Ocean (down to 4000 m-depth; Koike and Nagata,1997). These authors used high concentrations of MUF-P (250 µM, concentration kinetics from 0.6 to 1200 µM and 150 µM, respectively) that could stimulate ectoenzymes of cells attached on suspended or sinking particles, and thus adapted to face higher concentration ranges. However, these trends were also obtained using low concentrations (max 5 µM MUF-P), at depths down to 3500 m in the Tyrrhenian Sea (Tamburini et al., 2009). In the bathypelagic layers of the central Pacific, AP rates accounted for as much as half of those observed in the epipelagic layer but the < 0.2 µm dissolved AP was not included in the AP measurements (Koike and Nagata, 1997). These authors suggested that the deep-sea AP is due to fragmentation and dissolution of rapidly sinking particles. Indeed, it has been shown that AP determined on concentrated particles had the highest concentration factor compared to the AP of bulk seawater among different tested enzymes (Smith et al., 1992). Note, however, that our data generally stops in mesopelagic layers (1000 m). Tamburini et al. (2002) obtained a different relative contribution of deep-sea samples when using MUF-P concentrations of 25 nM or 5 µM at the DYFAMED station in the NW Mediterranean Sea (down to 2000 m-depth), further showing the artefact of concentration used. Furthermore, the deep activities could be x1.4 to x2.6 times higher due to the effect of hydrostatic pressure when not in the convective periods. We could not conclude that there was a systematic increase of specific AP with depth. Specific AP decreased at 5 stations, increased in 3 other stations and at the 2 remaining stations specific Vm increased based on Vm_{all}, but decreased based on Vm_1 (Fig. 9b). Note that for the deepest layers sampled (FAST: 2500 m and ION: 3000 m), results are also contrasting since specific AP decreases with depth at ION but increases at FAST. The particulate matter C/P ratio did not change with depth. However, the variability in the trend with depth seen for specific AP was also observed with DOC/DOP ratio. We expected to see an increase with depth due to a preferential removal of P, however, it was not systematic.

LAP enzymatic systems showed more differences and different trends with depth, than AP, Vm_{all} decreased with depth more intensively than Vm_1, but cell-specific LAP showed contradictory results: at all stations cell-specific Vm_1 decreases with depth (according to the DVF criterion, Fig. 9a) whereas Vm_{all} remained stable (2 stations over 10) or increased with depth (5 stations over 10). Using a high concentration of MCA-leu other authors have systematically found an increase in LAP activity per cell with depth in bathypelagic layers (Zaccone et al., 2012; Caruso et al., 2013).

The use of a large concentration set also impacts the Km values, because if only a high concentration range is used, the kinetic contribution of any enzyme with high affinity would be hidden. Baltar et al. (2009b), using a concentration of substrates ranging from 0.6 to 1200 µM, reported an increase in the LAP Km (~400 to 1200 µM) and AP Km (~2 to 23 µM) with depths down to 4500 m in the sub-tropical Atlantic. In contrast, Tamburini et al. (2002), using a concentration of substrates ranging from 0.05 to 50 µM, obtained lower Km values (ranging between 0.4 and 1.1 µM) for LAP in the Mediterranean deep waters (down to 2000 m depth). It is however difficult to come to a conclusion about the effect of the concentration on Km variability with depth by comparing 2 studies from different environments and using different sets of substrate concentrations. In our study where both kinetics were determined in the same waters, Km_{all} in particular, increased with depth more than Km_1, and the ratio Km_{all}/Km_1 switched from ~16 in

epipelagic waters to 121 and 316 in LIW and MDW layers, respectively. From our data set, among the two parameters LAP Vm and LAP Km, it is LAP Km which showed the greatest differences between the 2 types of kinetics. At many stations (TYR, ION, FAST and ST10), LAP Km_1 was stable or decreased with depth whereas LAP Km_{all} increased, suggesting that within deep layers LAP activity was linked more to the availability of suspended particles or fresh organic matter associated to sinking material, than to DON. Thus, the difference between Km_1 and Km_{all} might reflect a strategy to adapt to a potential spatial and/ or temporal patchiness in the distribution of suspended particles. Freshly sinking material is statistically not included in the bulk, because of the small volume of water incubated, but could contribute to the release of free bacteria, small suspended particles and DOM within its associated plume (Azam and Long, 2001; Tamburini et al., 2003; Grossart et al., 2007; Fang et al., 2014). Baltar et al. (2009a) also suggested that hot spots of activity at depth were associated with particles. The fact that the C/N ratio of particulate material increased (from 11-12 to 22-25) but not that much for DOC/DON (13-12 to 14-15 from SURF and DCM to LIW and MDW, respectively) confirms a preferential utilization of protein substrates from particles. Recently, Zhao et al. (2020) suggested that deep-sea prokaryotes and their metabolism are likely associated with particles rather than on the utilization of ambient-water DOC, based on the increasing contribution of genes encoding the secretory enzymes. Conversely to AP results, the higher differences between the 2 LAP enzymatic systems, suggest that microorganisms expressing LAP activity faced large gradients of protein concentrations and were adapted to pulsed inputs of particles.

4.3 How the set of concentrations used affects interpretation of enzymatic properties as indicators of nutrient imbalance of DOM quality and stoichiometry.

In epipelagic waters, both AP maximum rates (Vm_1, Vm_{all}) significantly increased by around 3 fold from the Algerian/Ligurian Basins to the Tyrrhenian Basin (t test, $p = 0.002$ and $p = 0.02$, respectively) and reached maximum values at ION. This longitudinal increase in AP activity was also confirmed by calculating specific activities which also increased towards ION. This increase of cell-specific AP appears to follow a decrease in DIP availability. While DIP can be assimilated directly through a high affinity absorption pathway, the assimilation of DOP requires its mineralization to free DIP which is then assimilated. POP is an indicator of living biomass and enzyme producers, but the correlation between VmAP and POP were negative in the surface layers (log-log relationship, $r = - 0.86$, -0.88 for Vm_{all} and Vm_1, respectively), suggesting that POP reflected the progressive eastward decline of living biomass and its increased capacity to derepress AP genes. VmAP rates in the surface did not correlate with DIP, however the relative DIP deficiency increased eastward, suggested by the deepening of the phosphacline (Table 1), the decrease in average DIP concentrations within the phosphate-depleted layer and the decrease in P diffusive fluxes reaching the surface layer (Pulido-Villena et al. 2020, in prep, this issue). Along a trans-Mediterranean transect, Zaccone et al. (2012), did not observe a trend between DIP and AP, although they also found also increased values of AP specific activities in the Eastern Mediterranean Sea. Bogé et al. (2012), using a concentration set close to ours (0.03-30 µM MUF-P) obtained differences in Vm for the 2 types of kinetics (contrary to our results) and described different relationships with DOP and DIP according to the low and high affinity enzymes. Such differences could be due to the large gradient of trophic conditions in their study, which studied an eutrophic bay where DOP and DIP concentration ranged from 0 to 185 nM, and from 0 to 329 nM, respectively. In order to circumvent the effect of depth, correlations are described in our study only for 10 surface data where the DIP concentration range is narrow (4 - 17 nM).

The AP/LAP ratio can be used as an indicator of N - P imbalance as demonstrated in enrichment experiments (Sala et al.2001). In this study using high concentrations of substrates (200 µM) the authors described a decrease in the AP/LAP ratio following DIP addition and, conversely, a large increase (10-fold) after the addition of 1 µM nitrate. In their initial experimental conditions, the ratio ranged from 0.2 to 1.9. We observed a similar low ratio in the western Mediterranean Sea, but in the Ionian Sea the AP/LAP reached 17 (Vm_{all}) and 43 (Vm_1), suggesting that nutrient stresses and imbalances can be as important and variable in different regions of the Mediterranean Sea, as observed after manipulation of nutrients. We have shown that such imbalances are more visible when using a low range of concentrations.

LAP/βGLU ratio is used as an index of the ability of marine bacteria to preferentially metabolize proteins rather than polysaccharides. Within epipelagic layers, the prevalence of LAP over βGLU is a recurrent observation in temperate areas (Christian and Karl, 1995; Rath et al., 1993) and in high latitudes (Misic et al., 2002, Piontek et al., 2014). For example, LAP/βGLU ratio varied widely from the Equator to the Southern Ocean, with values from 0.28 - 593 (Sinsabaugh and Shah, 2012). In the Ross Sea, this ratio exhibited a relationship with primary production (Misic et al., 2002). In the Caribbean Sea, along an eutrophic to oligotrophic gradient, the LAP/βGLU ratio increased toward oligotrophy (Rath and Herndl, 1993). In the epipelagic zone, during our study, the degree of trophic conditions exhibited a small gradient of productivity (18 to 35 mg TChla m^{-2}) along the Western to the Eastern Mediterranean Sea. Following this gradient, LAP /βGLU ratio ranged from 3 to 17 for Vm_{all}, and from 8 to 34 for Vm_1 and thus varied according to the concentration range tested, in agreement with previous reported ratios (10 and 20 for the low concentration and high concentration range, respectively; Unanue et al., 1999). Finally, the LAP/βGLU ratios reported in this study and other work using low substrate ranges are still lower than when using higher concentrations: 20-200 in the subarctic Pacific (Fukuda et al., 1995, using 200 µM concentration), 213 at station ALOHA in the equatorial Pacific (Christian and Karl, 1995, using L-leucyl-β–naphtylamine instead of MCA-leu at 1000 µM and MUF-βGLU at 1.6 µM), suggesting that the ratio LAP/βGLU is highly variable according to the fluorogenic substrate concentration and not in a regular way. As observed for the AP/LAP ratio, the LAP/βGLU ratio showed exacerbated variations when using the low affinity enzyme over the high affinity enzyme.

Throughout the water column, variations in the relative activity of different enzymes is also suggested as a possible indicator of changes in bacterioplankton nutrition patterns. The LAP/βGLU ratio decreased with depth, following the decrease in the protein to carbohydrate ratio of particulate material (Misic et al., 2002), nitrogen being re-mineralized faster than carbon. However, here the TAA-C/TCHO-C ratio was consistently higher within the DCM layer (~90 m) than at the surface and the LAP/βGLU ratio of both Vm_1 and Vm_{all} increased as a consequence, revealing important DON cycling (relative to DOC) at the DCM in comparison to what occurred in the mixed layers. Below the DCM layer, the particulate C/N ratio increased with depth and TAA-C /TCHO-C decreased, likewise supporting a faster hydrolysis of N organic sources than C organic sources. We estimated Vm_{all} LAP/Vm_{all} βGLU ratios from a few of the single rates measured at high concentration (most βGLU kinetics at depth were not available), and observed, in contrast to Misic et al (2002), an increase of the ratio within deep layers, as βGLU decreased faster than LAP with depth. A bias could be due to the absence of βGLU kinetics at depth, nevertheless other authors have also shown an increase of LAP/βGLU ratio with depth (Hoppe and Ullrich, 1999 in Indian Ocean, Placenti et al., 2018 in the Ionian Sea).

4.4 How the set of concentration used affects potential contribution of macromolecules hydrolysis to bacterial production

Our results clearly showed the influence of the concentration set used to compute *in situ* hydrolysis rates**.** TAA concentrations were lower than Km_1 and Km_{all}. The two Michaelis–Menten plots cross each other, at a substrate value of about 1.8 ± 1.3 µM for LAP and 1.7 ± 0.6 µM for βGLU. Considering the TAA range, and the high affinity enzyme (Km_1 Vm_1) with its low Km and high turnover rates, *in situ* rates are consequently higher using the high affinity enzyme kinetics. Although TCHO ranges were lower than Km_1 but higher than Km_{all}, TCHO was always lower than the crossing concentration point of the two types of kinetics, and consequently, again, the use of kinetic parameters of the high affinity enzyme lead to higher *in situ* hydrolysis rates than when using those of the low affinity enzyme. If the experimentally added substrate concentration is clearly above the possible range of concentrations found in the natural environment *in situ* rates could be largely overestimated. To obtain a significant determination of the *in situ* rates, the added substrate concentrations should be close to the range of variation expected in the studied environment (Tamburini et al., 2002).

We compared the *in situ* LAP hydrolysis rates to the N demand of heterotrophic prokaryotes (which was based on bacterial production data assuming C/N ratio of 5, with no active excretion of nitrogen), and the in situ rates of TAA plus TCHO to the bacterial carbon demand (based on a bacterial growth efficiency of 10% (Gazeau et al, this issue, in prep, Céa et al., 2014, Lemée et al., 2002). Using the low affinity enzyme constants (Vm_{all} and Km_{all}), hydrolysis of TAA by LAP contributed only to 25% ± 22% of the bacterial N demand in epipelagic layers and 26% ± 24% in deep layers. This contribution increased using the high affinity enzyme constants (48% ± 29% and 180% ± 154 % in epipelagic layers and deep layers, respectively). In the North Atlantic, the contribution of LAP hydrolysis rates of particles (0.3 µM MCA-leucine added) to bacterial nitrogen demand varied between 63 and 87%, increasing at 200 m. Crottereau and Delmas (1998) combined kinetics of LAP with combined amino-acid concentrations and found a range of 6-121% contribution to bacterial N demand in aquatic eutrophic ponds. A large variability of LAP hydrolysis contribution to bacterial N demand has also been detected in coastal-estuarine environments using a radiolabeled natural protein as a substrate (2 - 44%, Keil and Kirchman, 1993). Pointek et al. (2014) used the turnover of βGLU and LAP determined with 1 µM analog substrate concentrations to compute in situ TCAA and TCHO hydrolysis rates along a 79°N transect in the North Atlantic and showed that 134% and 52% of BP could be supported by peptide and polysaccharides hydrolyzed by enzyme activities, respectively. Based on a bacterial growth efficiency of 10%, these fluxes will represent 10 times less, i.e. 13 and 5 % of bacterial carbon demand, which is in the order of magnitude that we obtained. In our study, the contribution of TAA hydrolysis to bacterial N demand is increasing within the DCM compared to the SURF layer (from means of 10 to 40% based on the high affinity enzyme). This is consistent, however, as some cyanobacteria can also express LAP (Martinez and Azam, 1993) and *Synechococcus* and *Prochlorococcus* are dominant phytoplankton groups in the Mediterranean Sea (Siokou-Frangou et al., 2010). In our study, the DCM was an active biomass layer where primary production (PP) peaked (Marañón et al., 2020). Size fractionation of primary production showed the importance of the phytoplankton excretion, which contributed between 20 to 55% of the total PP depending on stations (Marañón et al, 2020). Within the surface mixed layer, other sources of N such as atmospheric deposition could sustain a significant part of bacterial N demand. The dry atmospheric

deposition (inorganic+ organic) of N at all stations within the PEACETIME cruise corresponded to 25 ± 17% of bacterial N demand (Van Wambeke et al, 2020).

Likewise, the *in situ* cumulated hydrolysis rates of TCHO by βGLU, estimated only in epipelagic layers were ~3 times higher using the high affinity enzyme. We summed C sources coming from the hydrolysis by LAP and by βGLU in epipelagic layers (Fig. 11) and compared them to the bacterial carbon demand. Dissolved proteins and combined carbohydrates contributed to only a small fraction of the bacterial carbon demand: 1.5% based on the low affinity enzyme and 3 % based on the high affinity enzyme.

It is only within deeper layers that the hydrolysis rates of TAA at some stations were more important than bacterial N demand, suggesting that proteolysis is one of the major sources of N for heterotrophic bacteria in aphotic layers. However, this was only based on the Vm_1 and Km_1 kinetic parameters (i.e. the high affinity enzyme) where we found cases of over-hydrolysis of organic nitrogen (Fig. 10). This over-hydrolysis was particularly marked in the LIW water mass of the Tyrrhenian Basin, in which over-hydrolysis up to 220% was obtained as well as higher TAA concentrations in comparison to 'older' LIW waters in the Algerian Basin. TAA decreased faster than DON along the LIW trajectory, so that the labile DON fraction (combined amino acids) was degraded first. Sinking particles or large aggregates associated with attached bacteria are considered to be major providers of labile organic matter for free bacteria (Smith et al., 1992). We could consider that with the 5 mL volume of water hydrolyzed for TAA analysis, and the 2 mL water volume used to determine ectoenzymatic kinetics, most of this particulate detrital pool of big size or big density (i.e. fast sinking particles) is underrepresented, and thus the contribution of TAA hydrolysis to bacterial nitrogen demand is underestimated. However, there is an increasing evidence of release from particles not only of monomers issued from hydrolysis, but also of ectoenzymes produced by deep-sea prokaryotes attached on particles themselves (Zhao et al., 2020). This could explain why, in a small volume of bulk sea water sample not representative of big or fast sinking particles, we still observe multiple kinetics. Studying alkaline phosphatase activity in the Toulon Bay, Bogé et al. (2013) observed biphasic kinetics only in the dissolved phase, which also suggests that AP low affinity enzyme originates from enzyme secretion from particles. Afterwards, this team focused their research by size fractionation of particulate material and they found that the origin of the low affinity enzyme was mostly due to the > 90 µm fraction, i.e. big particles (Bogé et al., 2017).

5 Conclusions

Vertical and regional variability of activities were shown in the Mediterranean Sea, where heterotrophic prokaryotes face not only carbon, but also N and P limitations. Although biased by the use of artificial fluorogenic substrates, ectozenzymatic activity is an appropriate tool to study the adaptation of prokaryotes to the large gradients in stoichiometry, chemical characteristics and quantities of organic matter they face, especially when using high concentrations. We have shown that the debates about relative increases or decreases of Vm or specific activities per depth are largely related to the choice of concentration set used. The ratio AP/LAP or LAP/βGLU used to track nutrient imbalances of DOM quality changes showed larger ranges of variation using low rather than large affinity enzymes. Finally, to obtain a significant determination of *in situ* rates, the added substrate concentrations should be close to the range of variation expected in the studied environment. While the use of microplate titration technique greatly improved the simultaneous study of different EEAs, further assessments of enzymatic kinetics should be performed

785 systematically in enzymatic studies. Future combination of such techniques with the chemical identification of DOC and DON pools, and meta-omics, as well as the use of marine snow catchers, will help our understanding of the biodegradation of organic matter in a 'sea of gradients'.

Data availability

Data will be accessible once the special issue is published at the French INSU/CNRS LEFE
790 CYBER database: http://www.obs-vlfr.fr/proof/php/PEACETIME/peacetime.php, last access: 29 October 2020. Scientific coordinator: Hervé Claustre; data manager, webmaster: Catherine Schmechtig. The policy of the database is detailed here: http://www.obs-vlfr.fr/proof/dataconvention.php (last access: 29 October 2020).

Author contribution

795 FVW and CT designed the study. FVW, CT, MG and SG sampled and incubated samples for ectoenzymatic activity on board, FVW and SG analyzed the ectoenzymatic data. FVW and MG sampled and analyzed BP samples, BZ sampled and analyzed TAA and TCHO samples, AE managed the TCHO an TAA analysis and treatments, EP and KD sampled and analyzed DIP analysis with the LWCC technique, SN sampled and analyzed nutrients and organic matter, VT
800 assisted in CTD operations and analyzed water masses, JD sampled for DOC and flow cytometry, PC analyzed bacterial abundances, BM analyzed DOC, FVW prepared the ms with contribution from all co-authors.

Competing interests

The authors declare that they have no conflict of interest

805 Special issue statement

This article is part of the special issue 'Atmospheric deposition in the low-nutrient–low-chlorophyll (LNLC) ocean: effects on marine life today and in the future (ACP/BG inter-journal SI)'. It is not associated with a conference

Financial support

810 This study is a contribution of the PEACETIME project (http://peacetime-project.org), a joint initiative of the MERMEX and ChArMEx components supported by CNRS-INSU, IFREMER, CEA, and Météo-France as part of the programme MISTRALS coordinated by INSU (doi: 10.17600/17000300).

Acknowledgements: The authors thank also many scientists & engineers for their assistance with
815 sampling/analyses: J Ras for TCHO, R Flerus for TAA, J Guittoneau for nutrients, T Blasco for POC, J Uitz and C Dimier for Chl a (analysed at the SAPIGH HPLC analytical service at the IMEV, Villefranche), I Obernosterer for DOC. We warmly thank C Guieu and K Deboeufs, as coordinators of the program PEACETIME. We are grateful to the two anonymous reviewers and editor C Klass for their constructive and pertinent comments.

820

References

Aminot, A. and Kérouel, R.: Dosage automatique des nutriments dans les eaux marines,in:Méthodes d'analyses en milieu marin, edited by: IFREMER, 188 pp, 2007.

Aluwihare, L. I., Repeta, D. J., and Chen, R. F.: A major biopolymeric component to dissolved organic carbon in surface sea water, Nature, 387, 166–169. doi : 10.1038/387166a0, 1997.
Arnosti, C.: Microbial Extracellular enzymes and the marine carbon cycle, Ann. Rev. Mar. Sci., 3, 401-425, 2011.
Arrieta, J. M. and Herndl, G. J.: Assessing the diversity of marine bacterial β-glucosidases by capillary Electrophoresis Zymography, Appl. Environ. Microb., 67, 4896-4900, 2001.
Azam, F., and Long, R. A. (2001). Sea snow microcosms, Nature, 414, 495-498.
Azzaro, M., La Ferla, R., Maimone, G., Monticelli, L. S., Zaccone, R., and Civitarese, G.: Prokaryotic dynamics and heterotrophic metabolism in a deep convection site of Eastern Mediterranean Sea (the Southern Adriatic Pit), Cont. Shelf Res., 44, 06-118, doi: 10.1016/j.csr.2011.07.011, 2012.
Baklouti, M., Diaz, F., Pinazo, C., Faure, V., and Quéguiner, B.: Investigation of mechanistic formulations depicting phytoplancton dynamics for models of marine pelagic ecosystems and description of a new model, Prog. Oceanogr., 71, 1–33, doi:1016/j.pocean.2006.05.002, 2006.
Baltar, F., Arístegui, J., Gasol, J. M., Sintes, E., and Herndl, G. J.: Evidence of prokaryotic metabolism on suspended particulate organic matter in the dark waters of the subtropical North Atlantic, Limnol. Oceanogr., 54, 182-193, doi:10.4319/lo.2009.54.1.0182, 2009a.
Baltar, F., Aristegui, J., Sintes, E., van Aken, H. M., Gasol, J. M., and Herndl, G. J.: Prokaryotic extracellular enzymatic activity in relation to biomass production and respiration in the meso- and bathypelagic waters of the (sub)tropical Atlantic, Env. Microbiol., 11, 1998–2014, 2009b.
Baltar, F.: Watch Out for the "Living Dead": Cell-Free Enzymes and Their Fate, Front. Microbiol., 8, article 2438, doi: 10.3389/fmicb.2017.02438,2018.
Bogé G., Lespilette, M., Jamet, D., and Jamet, J-L.: Role of sea water DIP and DOP in controlling bulk alkaline phosphatase activityin N.W. Mediterranean Sea (Toulon, France), Mar.Pollut.Bull., 64, 1989-1996, doi: 10.1016/j.marpolbul.2012.07.028, 2012.
Bogé, G., Lespilette, M., Jamet, D. and Jamet, J.-L.: The relationships between particulate and soluble alkaline phosphatase activities and the concentration of phosphorus dissolved in the seawater of Toulon Bay (NW Mediterranean). Mar. Pollut. Bull., 74, 413-419, doi: 10.1016/j.marpolbul.2013.06.003, 2013.
Bogé, G., Lespilette, M., Jamet, D., and Jamet, J.-L.: Role of DOP on the alkaline phosphatase activity of size fractionated plankton in coastal waters in the NW Mediterranean Sea (Toulon Bay, France), Mar. Pollut. Bull., 117, 264-273, doi:10.1016/j.marpolbul.2016.11.037, 2017.
Caruso, G., Monticelli, L., La Ferla, R., Maimone, G., Azzaro, M., Azzaro, F., Decembrini, F., De Pasquale, F., Leonardi, M., Raffa, F., Zappal, G., and De Domenico, E.: Patterns of Prokaryotic Activities and Abundance among the Epi-Meso and Bathypelagic Zones of the Southern-Central Tyrrhenian Sea, Oceanography, 1, 1, doi: 10.4172/ocn.1000105, 2013.
Cauwet, G.: Determination of dissolved organic carbon (DOC) and nitrogen (DON) by high temperature combustion, in: Methods of Seawater analysis, edited by: Grashoff, K., Kremling,K. and Ehrhard, M., 3rd Ed., Wiley-VCH, Weinheim, 407-420, 1999.
Céa, B., Lefèvre, D., Chirurgien, L., Raimbault, P., Garcia, N., Charrière, B., Grégori, G., Ghiglione, J.-F., Barani, A., Lafont, M., and Van Wambeke, F.: An annual survey of bacterial production, respiration and ectoenzyme activity in coastal NW Mediterranean waters: temperature and resource controls, Environ Sci. Pollut. Res., doi: 10.1007/s11356-014-3500-9, 2014.
Christian, J. R. and Karl, D. M.: Bacterial ectoenzymes in marine waters: Activity ratio and temperature responses in three oceanographic provinces, Limnol. Oceanogr., 40, 1046-1053, 1995.
Chróst, R.J. Microbial enzymes in aquatic environments, Springer-Verlag, New York, 1991.
Dittmar, T.H., Cherrier, J. and Ludwichowski, K.-U: The analysis of amino acids in seawater. In: Practical Guidelines for the Analysis of Seawater, edited by: Wurl, O., Boca Raton, FL: CRC-Press, 67–78, 2009.
Engel, A., and Händel, N.: A novel protocol for determining the concentration and composition of sugars in particulate and in high molecular weight dissolved organic matter (HMW-DOM) in seawater. Mar. Chem. 127, 180–191, 2011

Fang, J., Zhang, L., Li, J., Kato, C., Tamburini, C., Zhang, Y., Dang, H., Wang, G., & Wang, F.: The POM-DOM piezophilic microorganism continuum (PDPMC)—The role of piezophilic microorganisms in the global ocean carbon cycle, Science China (Earth Sciences), 1–10, doi:10.1007/s11430-014-4985-2, 2014.

Gazeau, F., Van Wambeke, F., Marañón, E., Pérez-Lorenzo, M., Alliouane, S., Stolpe, C., Blasco, T., Zäncker, B., Engel, A., Marie, B., Guieu, C.: Impact of dust enrichment on carbon budget and metabolism of Mediterranean plankton communities under present and future conditions of pH and temperature, Biogeosciences Discuss., in prep., this issue.

Grossart, H.-P., Tang, K. W., Kiørboe, T., and Ploug, H.: Comparison of cell-specific activity between free-living and attached bacteria using isolates and natural assemblages, FEMS Microb. Lett., 266, 194–200, doi:10.1111/j.1574-6968.2006.00520.x, 2007.

Guieu, C., D'Ortenzio, F., Dulac, F., Taillandier, V., Doglioli, A., Petrenko, A., Barrillon, S., Mallet, M., Nabat, P., and Desboeufs, K.: Introduction: Process studies at the air-sea interface after atmospheric deposition in the Mediterranean Sea - objectives and strategy of the PEACETIME oceanographic campaign (May–June 2017), Biogeosciences, 17, 5563-5585, doi:10.5194/bg-17-5563-2020, 2020.

Guyennon, A., Baklouti, M., Diaz, Palmiéri, J., Beuvier, J., Lebeaupin-Brossier, C., Arsouze, T., Beranger, K., Dutay, J.-C., and Moutin, T.: New insights into the organic carbonexport in the Mediterranean Sea from 3-D modeling, Biogeosciences, 12, 25-7046, doi: 10.5194/bg-12-7025-2015**,** 2015.

Hopkins, T. S.: Physical processes in the Mediterranean Basin. Estuarine transport processes, B. Kjerfve, editor, University of South Carolina, 269-310, 1978.

Hoppe, H.-G.: Significance of exoenzymatic activities in the ecology of brackish water: measurements by means of methylumbelliferyl-substrates, Mar. Ecol. Prog. Ser., 11, 299-308, 1983.

Hoppe, H.-G. and Ullrich, S.: Profiles of ectoenzymes in the Indian Ocean: phenomena of phosphatase activity in the mesopelagic zone, Aquat. Microb. Ecol., 19, 139-148, 1999.

Hoppe, H.-G., Ducklow, H., and Karrasch, B.: Evidence for dependency of bacterial growth on enzymatic hydrolysis of particulate organic matter in the mesopelagic ocean, Mar. Ecol. Prog. Ser,, 93, 277-283, 1993.

Keil, R.G, and Kirchman, D.:Dissolved combined amino acids: Chemical form and utilization by marine bacteria, Limnol. Oceanogr., 38: 1256-1270, 1993

Kirchman, D. L.: Leucine incorporation as a measure of biomass production by heterotrophic bacteria. In: Handbook of methods in aquatic microbial ecology,edited by: Kemp, P.F., Sherr, B.F., Sherr, E.B. and Cole, J.J., Lewis, Boca Raton, 509-512, 1993.

Koch, A.L. Oligotrophs versus copiotrophs, BioEssays, 23, 657–661, 2001.

Koike, I. and Nagata, T.: High potential activity of extracellular alkaline phosphatase in deep waters of the central Pacific, Deep-Sea Res. PT II, 44, 2283-2294, 1997.

Kress, N., Manca, B., Klein, B. and Deponte, D.: Continuing influence of the changed thermohaline circulation in the eastern Mediterranean on the distribution of dissolved oxygen and nutrients: Physical and chemical characterization of the water masses, J. Geophys. Res. Oceans, 108, 8109, doi:10.1029/2002JC001397,2003.

Krom, M. D., Herut, B. andMantoura, R. F. C.: Nutrient budget for the eastern Mediterranean: Implication for phosphorus limitation, Limnol. Oceanogr, 49, 1582-1592, doi:10.4319/lo.2004.49.5.1582, 2004.

Lascaratos, A., Roether, W., Nittis, K., and Klein, B.: Recent changes in deep water formation and spreading in the eastern Mediterranean Sea: a review, Prog. Oceanogr., 44, 5–36, 1999.

Lemée, R., Rochelle-Newall, E., Van Wambeke, F., Pizay, M.-D., Rinaldi, P., and Gattuso, J.-P.: Seasonal variation of bacterial production, respiration and growth efficiency in the open NW Mediterranean Sea., Aquat. Microb. Ecol., 29, 227-237, 2002

Lindroth, P., and Mopper, K.: High performance liquid chromatographic determination of subpicomole amounts of amino acids by precolumn fluorescence derivatization with o-phthaldialdehyde. Anal. Chem. 51, 1667–1674, 1979

Malanotte-Rizzoli P., Manca, B.B., Marullo,S., Ribera d'Alcalà,M., Roether, W., Theocharis, A. and Conversano, F.:The Levantine Intermediate Water Experiment (LIWEX) Group: Levantine basin - A laboratory for multiple water mass formation processes, J. Geophys. Res-Oceans, 108, doi:10.1029/2002JC001643, 2003.

Marañón, E., Van Wambeke, F., Uitz, J., Boss, E.S., Pérez-Lorenzo, M., Dinasquet, J., Haëntjens, N., Dimier, C., Taillandier, V.: Deep maxima of phytoplankton biomass, primary production and bacterial production in the Mediterranean Sea during late spring, Biogeosciences Discuss., https://doi.org/10.5194/bg-2020-261, in review, 2020.

Martinez, J. and Azam, F.: Aminopeptidase activity in marine chroococcoid cyanobacteria. Appl. Environ. Microb., 59, 3701-3707, 1993.

Martinez, J., Smith, D. C., Steward, G. F., and Azam, F.: Variability in ectohydrolytic enzyme activities of pelagic marine bacteria and its significance for substrate processing in the sea, Aquat. Microb. Ecol., 10, 223-230, 1996.

Misic, C., Povero, P., and Fabiano, M.: Ectoenzymatic ratios in relation to particulate organic matter distribution (Ross Sea, Antarctica), Microb. Ecol., 44, 224-234, doi:10.1007/s00248-002-2017-9, 2002.

Piontek, J., Sperling, M., Nothig, E.-V., and Engel, A.: Regulation of bacterioplankton activity in Fram Strait (Arctic Ocean) during early summer: The role of organic matter supply and temperature, J. Marine Syst., 132, 83-94, doi: 10.1016/j.jmarsys.2014.01.003, 2014.

Placenti, F., Azzaro, M., Artale, V., La Ferla, R., Caruso, G., Santinelli, C., Maimone, G., Monticelli, L. S., Quinci, E. M., and Sprovieri, M.: Biogeochemical patterns and microbial processes in the Eastern Mediterranean Deep Water of Ionian Sea, Hydrobiologia, 815, 97-112, doi: 10.1007/s10750-018-3554-7, 2018.

Pulido-Villena, E., Van Wambeke, F., Desboeufs, K., Petrenko, A., Barrillon, S., Djaoudi, K., Doglioli, A., D'Ortenzio, F., Fu, Y., Gaillard, T., Guasco, S., Nunige, S., Raimbault, P., Taillandier, V., Triquet, S., Guieu, C. Analysis of external and internal sources contributing to phosphate supply to the upper waters of the Mediterranean Sea (Peacetime cruise), in prep for Biogeosciences, special issue PEACETIME.

Raimbault, P., Pouvesle W., Diaz F., Garcia N., Sempere, R.: Wet-oxidation and automated colorimetry for simultaneous determination of organic carbon, nitrogen and phosphorus dissolved in seawater, Mar. Chem. 66, 161-169, 1999.

Rath, J., and Herndl, G. J.: Characteristics and Diversity of ß-D-Glucosidase (EC 3.2.1.21) Activity in Marine Snow, Appl. Environ. Microbiol., 60, 807-813, 1994.

Sala, M. M., Karner, M., Arin, L., and Marrassé, C.: Measurement of ectoenzyme activities as an indication of inorganic nutrient imbalance in microbial communities, Aquat. Microb. Ecol., 23, 301-311, doi:10.3354/ame023301, 2001.

Severin, T., Sauret, C., Boutrif, M., Duhaut, T., Kessouri, F., Oriol, L., Caparros, J., Pujo-Pay, M., Durrieu de Madron, X., Garel, M., Tamburini, C., Conan, P., and Ghiglione, J. F.: Impact of an intense water column mixing (0–1500 m) on prokaryotic diversity and activities during an open-ocean convection event in the NW Mediterranean Sea, Environ. Microbiol., 18, 4378-4390, doi:10.1111/1462-2920.13324, 2016.

Siokou-Frangou, I., Christaki, U., Mazzocchi, M. G., Montresor, M., Ribera d'Alcala, M., Vaque, D., and Zingone, A.: Plankton in the open Mediterranean Sea: a review, Biogeosciences, 7, 1543-1586, doi:10.5194/bg-7-1543-2010, 2010.

Stocker, R.: Marine Microbes See a Sea of gradients, Science, 38, 628-633,2012.

Sharp, J. H.: Improved analysis for "particulate" organic carbon and nitrogen from seawater, Limnol.Oceanogr.,19, 984-989, 1974.

Schroeder, K, Cozzi S, Belgacem, M, Borghini, M, Cantoni, C, Durante, S, Petrizzo, A, Poiana, A and Chiggiato, J. (2020) Along-Path Evolution of Biogeochemical and Carbonate System Properties in the Intermediate Water of the Western Mediterranean, Front. Mar. Sci. 7:375. doi: 10.3389/fmars.2020.00375, 2020.

Simon, M., Grossart, H., Schweitzer, B., Ploug, H.:Microbial ecology of organic aggregates in aquatic ecosystems, Aquat. Microb. Ecol. 28, 175-211, doi: 10.3354/ame028175, 2002.

Sinsabaugh, R. and Follstad Shah, J.: Ectoenzymatic Stoichiometry and Ecological Theory, Annu. Rev. Ecol., Evol. S., 43, 313-343, doi:10.1146/annurev-ecolsys-071112-124414, 2012.
Smith, D. C. and Azam, F.: A simple,economical method for measuring bacterial protein synthesis rates in sea water using 3H-Leucine, Mar. Microb. Food Webs, 6, 107-114, 1992.
Smith, D. C., Simon, M., Alldredge, A. L., and Azam, F.: Intense hydrolytic activity on marine aggregates and implications for rapid particle dissolution, Nature, 359, 139-142, 1992.
Taillandier, V., Prieur, L., D'Ortenzio, F., Riberad'Alcala, M., Pulido-Villena, E.: Profiling float observation of thermohaline staircases in the western Mediterranean Sea and impact on nutrient fluxes, Biogeosciences, 17, 3343–3366, doi: 10.5194/bg-17-3343-2020, 2020.
Tamburini, C., Garcin, J., Ragot, M., and Bianchi, A.: Biopolymer hydrolysis and bacterial production under ambient hydrostatic pressure through a 2000 m water column in the NW Mediterranean, Deep-Sea Res. PT II, 49, 2109–2123, doi:10.1016/S0967-0645(02)00030-9, 2002.
Tamburini, C., Garcin, J., and Bianchi, A.: Role of deep-sea bacteria in organic matter mineralization and adaptation to hydrostatic pressure conditions in the NW Mediterranean Sea, Aquat. Microb. Ecol., 32, 209–218. Doi: 10.3354/ame032209, 2003.
Tamburini, C., Garel, M., Al Ali, B., Mérigot, B., Kriwy, P., Charrière, B., and Budillon, G.: Distribution and activity of Bacteria and Archaea in the different water masses of the Tyrrhenian Sea, Deep Sea Res. PT II, 56, 700-714, doi: 10.1016/j.dsr2.2008.07.021, 2009.
Testor, P., Bosse, A., Houpert, L., Margirier, F., Mortier, L., Legoff, H., Dausse, D., Labaste, M., Kartensen, J., Hayes, D., Olita, A. Ribotti, A., Schroeder, K., Chiggiato, J., Onken, R., Heslop, R., Mourre, B., D'Ortenzio, F., Mayot, N., Lavigne, H., de Fommervault, O., Coppola, L., Prieur, L., Taillandier, V., Durrieu de Madron, X., Bourrin, F., Many, G., Damien, P., Estournel, C., Marsaleix, P., Taupier-Lepage, I., Raimbault, P., Waldman, R., Bouin, M-N., Giordani, H., Caniaux, G., Somot, S., Ducrocq, V. Conan P.: Multiscale observations of deep convection in the northwestern Mediterranean Sea during winter 2012–2013 using multiple platforms. J. Geophys.Res. Oceans, 123, 1745–1776. https://doi.org/10.1002/ 2016JC012671, 2018.
The Mermex Group. Marine ecosystems' responses to climatic and anthropogenic forcings in the Mediterranean. Prog. Oceanogr., 91(2), 97–166, doi: 10.1016/j.pocean.2011.02.003, 2011
Thingstad, T. F. and Rassoulzadegan, F.: Nutrient limitations, microbial food webs, and 'biological C-pumps': suggested interactions in a P-limited Mediterranean, Mar. Ecol. Prog. Ser., 117, 299-306, 1995.
Tholosan, O., Lamy, F., Garcin, J., Polychronaki, T., and Bianchi, A.: Biphasic extracellular proteolytic enzyme activity in benthic water and sediment in the North Western Mediterranean Sea, Appl. Environ. Microb., 65, 1619-1626, 1999.
Unanue, M., Azua, I., Arrieta, J. M.,Labirua-Iturburu, A., Egea, L., and Iriberri, J.: Bacterial colonization and ectoenzymatic activity in phytoplankton-derived model particles: Cleavage of peptides and uptake of amino acids, Microb. Ecol., 35, 136-146, doi: 10.1007/s002489900068, 1998.
Unanue, M., Ayo, B., Agis, M., Slezak, D., Herndl, G. J., andIriberri, J.: Ectoenzymatic activity and uptake of monomers inmarine bacterioplankton described by a biphasic kinetic model, Microb. Ecol., 37, 36–48, doi:10.1007/s002489900128,1999.
Van Wambeke, F., Christaki, U., Giannakourou, A., Moutin, T. and Souvemerzoglou, K.: Longitudinal and vertical trends of bacterial limitation by phosphorus and carbon in the Mediterranean Sea, Microb. Ecol., 43, 119-133, doi: 10.1007/s00248-001-0038-4, 2002.
Van Wambeke, F., Taillandier V., Desboeufs, K., Pulido-Villena, E., Dinasquet, J., Engel, A., Marañón, E., Ridame, C., Guieu, C.: Influence of atmospheric deposition on biogeochemical cycles in an oligotrophic ocean system, Biogeosciences Discuss., https://doi.org/10.5194/bg-2020-411, 2020
Wust, G.: On the vertical circulation of the Mediterranean Sea, J.Geophys. Res., 66, 10, 3261-3271, 1961
Zaccone, R., and Caruso, G.: Microbial enzymes in the Mediterranean Sea: relationship with climate changes, AIMS Microbiology, 5, 251-272, 2019.

Zaccone, R., Boldrin, A., Caruso, G., La Ferla, R., Maimone, G., Santinelli, C., and Turchetto, M.: Enzymatic Activities and Prokaryotic Abundance in Relation to Organic Matter along a West–East Mediterranean Transect (TRANSMED Cruise), Microb. Ecol., 64, 54-66, 2012.

Zhang, J.-Z. and Chi, J.:Automated analysis of nano-molar concentrations of phosphate in natural waters with liquid waveguide, Environ. Sci. Technol., 36, 1048-1053, doi:10.1021/es011094v, 2002.

Zhao, Z., Baltar, B., and Herndl, G. J.: Linking extracellular enzymes to phylogeny indicates a predominantly particle-associated lifestyle of deep-sea prokaryotes, Sciences Advances, 6, eaaz4354, https://doi.org/10.1126/sciadv.aaz4354, 2020.

Figure Legends

Figure 1. Sampling sites. Colour codes on dots correspond to the plots on Fig.2

Figure 2. Physical properties along the different stations: T/S diagram. Colour codes correspond to the stations mapped Fig. 1. Principal water masses are indicated. MAW: Modified Atlantic Waters, LIW: Levantine intermediate Waters, WMDW: Western Mediterranean Deep waters, EMDW: Eastern Mediterranean Deep Waters.

Figure 3. Example of Michaelis-Menten plots, DCM layer at station FAST. a, b, c: Dots are data, continuous lines the non linear regression plot derived from the global model (concentration set 0.025 to 50 µM) and dotted lines the plot derived from the model 50. d, e, f: Small graphs show dotted lines corresponding to regression plots derived from model 1 (concentration set 0.025-1 µM).

Figure 4. Relationships between kinetic parameters resulting from model 1, model 50 and global model for the three ectoenzyme (a, d: Leucine aminopeptidase (LAP), b, d: βglucosidase (βGLU), c, f : alkaline phosphatase (AP). a,b,c: relationships between Vm_1 and Vm_{all} and between Vm_{50} and Vm_{all}; d,e, f: relationships between Km_1 and Km_{all} and between Km_{50} and Km_{all}; and. Error bars show standard errors. The standard error of Km_{all} in the relationships between Km_{all} and Km_1 (in d, e, f, white dots) is not plotted for clarity. For all the other dots, when the error bar is not visible, it is included in the data dot.

Figure 5. Distribution of leucine aminopeptidase (LAP) kinetic parameters Vm (a) and Km (b) calculated from model 1 (Vm_1, Km_1) and global model (Vm_{all}, Km_{all}) The error bars are standard errors derived from the non linear regressions.

Figure 6. Distribution of βglucosidase (βGLU) kinetic parameters Vm (a) and Km (b) calculated from model 1 (Vm_1, Km_1) and global model (Vm_{all}, Km_{all}) in epipelagic layers SURF and DCM..The error bars are standard errors derived from the non linear regressions. Within LIW and MDW layers. kinetics were impossible to compute due to the low range of rates measurable (see results) and the black bar in a) is assumed to represent a minimal value for Vm_{all} .

Figure 7. Distribution of alkaline phosphatase (AP) kinetic parameters Vm (a) and Km (b) calculated from model 1 (Vm_1, Km_1) and global model (Vm_{all}, Km_{all}). The error bars are standard errors derived from the non linear regressions.

Figure 8. Box plot distributions of specific Vm_1 and Vm_{all} per bacterial cell, for alkaline phosphatase (a: per cell Vm_{all} AP, b: per cell Vm_1 AP) and leucine aminopeptidase (c: per cell Vm_{all} LAP, d: per cell Vm_1 LAP). Box limits 25% and 75% percentiles, horizontal bar is median, red cross is mean, blue dots are outliers.

Figure 9. Depth decreasing factor (DVF, unitless) among different specific activities. DVF is calculated as the mean of pooled data from SURF and DCM layers divided by the mean of pooled data from LIW and MDW layers. a: DVF of per cell leucine aminopeptidase (per cell Vm_{all}LAP and per cell Vm_1LAP); b: DVF of alkaline phosphatase (per cell Vm_{all}AP and per cell Vm_1AP); c: For β–glucosidase DVF, specific activities are based on the few detectable rates at high concentration (per cell VβGLU, yellow dots). Black crosses are specific heterotrophic prokaryotic production per cell (per cell BP).

Figure 10. *In situ* hydrolysis rates of dissolved proteins and particulate detrital N-proteins (nmol N L^{-1} h^{-1}), determined from LAP ectoenzyme kinetics Vm_1/Km_1 versus Vm_{all} Km_{all}, and comparison to heterotrophic bacterial nitrogen demand, determined from BP assuming a biomass C/N molar

ratio of 5 and no active excretion of nitrogen. a) epipelagic layers (SURF, DCM), b) deeper layers (LIW, MDW).

Figure 11. *In situ* hydrolysis rates of dissolved and particulate detrital carbohydrates and C-proteins (nmol C L^{-1} h^{-1}), determined from LAP and βGLU ectoenzymatic parameters Vm_1 & Km_1 versus Vm_{all} & Km_{all}, and comparison to heterotrophic bacterial carbon demand (BCD, determined from BP assuming a BGE of 10%) in epipelagic waters. Note the x10 scale for bacterial carbon demand on the right.

Table 1. Characteristics of the stations. Lat: Latitude, Long: Longitude, Bott D : bottom depth, T_{5m} : Temperature at 5m depth, Ncline depth : nitracline depth, calculated as the layer where NO3 reaches 50 nM; , Pcline depth : phosphacline depth, estimated as the layer where DIP reaches 50 nM; IChla: integrated total chlorophyll a, LIW D: depth of the LIW layer sampled, MDW D: depth of the MDW layer sampled

	sampling date	Lat °N	Long °E	Bott D m	T_{5m} °C	DCM D m	Ncline D m	Pcline D m	I Chl a mg m^{-2}	LIW D m	MDW D m
ST 10	6/8/2017	37.45	1.57	2770	21.6	89	30	69	28.9	500	1000
FAST	6/3/2017	37.95	2.92	2775	21.0	87	50	59	27.3	350	2500
ST 1	5/12/2017	41.89	6.33	1580	15.7	49	48	76	35.0	500	1000
ST 2	5/13/2017	40.51	6.73	2830	17.0	65	40	70	32.7	500	1000
ST 3	5/14/2017	39.13	7.68	1404	14.3	83	47	100	23.2	450	1000
ST 4	5/15/2017	37.98	7.98	2770	19.0	64	42	63	29.2	500	1000
ST 5	5/16/2017	38.95	11.02	2366	19.5	77	42	78	30.5	200	1000
TYR	5/17/2017	39.34	12.59	3395	19.6	73	82	95	31.3	200	1000
ST 6	5/22/2017	38.81	14.50	2275	20.0	75	43	113	18.7	400	1000
ION	5/25/2017	35.49	19.78	3054	20.6	105	85	231	27.7	250	3000

Table 2. Heterotrophic bacterial abundances (BA), bacterial production (BP) and ectoenzyme kinetic parameters of the global model (Vm_{all}, Km_{all}) obtained from the entire substrate range (0.025 to 50 µM) and model 1 (Vm_1, Km_1) obtained from the low substrate range (0.025 to 1 µM) for leucine aminopeptidase (LAP), β-glucosidase (βGLU) and alkaline phosphatase (AP) at the 4 layers. Means ± sd and range values given for all stations). Maximum velocity rates (Vm_{all} and Vm_1), half saturation constants (Km_{all} and Km_1). nk: No kinetic available as not enough significant rates to plot Michaelis-Menten kinetics.

		SURF	DCM	LIW	MDW
Vm_{all} LAP	mean ± sd	0.97 ± 0.79	1.20 ± 0.92	0.22 ± 0.18	0.15 ± 0.08
nmol l^{-1} h^{-1}	range	0.36 – 2.85	0.35 – 2.83	0.08 – 0.69	0.06 – 0.28
Vm_1 LAP	mean ± sd	0.29 ± 0.10	0.45 ± 0.25	0.028 ± 0.014	0.017 ± 0.010
nmol l^{-1} h^{-1}	range	0.21 – 0.56	0.19 – 0.98	0.014 – 0.060	0.007 – 0.042
Vm_{all} βGLU	mean ± sd	0.13 ± 0.04	0.11 ± 0.06	nk	nk
nmol l^{-1} h^{-1}	range	0.08 – 0.23	0.03 – 0.22		
Vm_1 βGLU	mean ± sd	0.019 ± 0.009	0.025 ± 0.019	nk	nk
nmol l^{-1} h^{-1}	range	0.012 – 0.040	0.014 – 0.077		
Vm_{all} AP	mean ± sd	2.52 ± 2.62	3.73 ± 4.52	0.38 ± 0.48	0.24 ± 0.40
nmol l^{-1} h^{-1}	range	0.30 – 8.30	0.11– 14.6	0.04 – 1.66	0.06 – 1.30
Vm_1 AP	mean ± sd	1.55 ± 1.58	3.01 ± 4.01	0.24 ± 0.33	0.12 ± 0.25
nmol l^{-1} h^{-1}	range	0.25–5.62	0.07–13.2	0.02 – 1.11	0.01 – 0.80
Km_{all} LAP	mean ± sd	6.0 ± 5.6	5.3 ± 7.6	16.4 ± 13.3	15.2 ± 11.3
µM	range	0.8–20.9	0.7–25.0	3.6 – 38.1	1.8 – 34.6
Km_1 LAP	mean ± sd	0.49 ± 0.18	0.43 ± 0.27	0.23 ± 0.19	0.13 ± 0.11
µM	range	0.12–0.70	0.07–0.90	0.10 – 0.69	0.01 – 0.39
Km_{all} βGLU	mean ± sd	10.6 ± 6.3	7.7 ± 5.1	nk	nk
µM	range	4.4–27.4	1.2–14.2		
Km_1 βGLU	mean ± sd	0.044 ± 0.071	0.11± 0.11	nk	nk
µM	range	0.009–0.244	0.01 – 0.36		
Km_{all} AP	mean ± sd	0.58 ± 0.67	0.49 ± 0.34	2.25 ± 2.42	2.6 ± 3.5
µM	range	0.09–2.18	0.18–1.07	0.17 – 7.32	0.4 – 11.9
Km_1 AP	mean ± sd	0.11 ± 0.03	0.27 ± 0.28	0.37 ± 0.22	0.27 ± 0.16
µM	range	0.07–0.14	0.05 – 0.80	0.14 – 0.89	0.06 – 0.52
BA	mean ± sd	5.3±1.6	5.4 ±1.5	1.13 ± 0.40	0.56 ± 0.15
10^5 cells ml^{-1}	range	2.1–7.8	4.0 – 8.5	0.41 – 1.91	0.33 – 0.78
BP	mean ± sd	37 ± 13	21±7	0.77 ±0.40	0.27 ± 0.19
ng C l^{-1} h^{-1}	range	26 – 64	12 – 32	0.39 – 1.60	0.07 – 0.60

Table 3. Turnovertimes of ectoenzymes (Km/Vm ratio). Means ± sd and range values given . for leucine aminopeptidase (LAP), beta glucosidase (βGLU), and alkaline phosphatase (AP). nk no kineticks, not enough rates to plot Michaelis Menten kinetics. The turnovertimes are calculated from the global model (Km_{all}/Vm_{all}) or the model 1 (Km_1/Vm_1).

	Units: days	SURF	DCM	LIW	MDW
Km_{all}/Vm_{all} LAP	mean ± sd	255 ± 79	158 ± 182	3394 ± 2629	4161 ± 1806
	range	94 – 340	40 – 663	1294 – 9016	1308 – 7028
Km_1/Vm_1 LAP	mean ± sd	74 ± 26	42 ± 22	345 ± 235	343 ± 298
	range	15 – 106	15 – 82	141 – 985	55 – 959
Km_{all}/Vm_{all} βGLU	mean ± sd	3464 ± 1576	3091 ± 1551	ld	ld
	range	1997-7395	328-5481	nd	nd
Km_1/Vm_1 βGLU	mean ± sd	126 ± 233	247 ± 273	ld	ld
	range	20-784	15-873	nd	nd
Km_{all}/Vm_{all} AP	mean ± sd	12 ± 9	39 ± 46	563 ± 542	914 ± 817
	range	2 – 33	0.7 – 113	16 – 1441	20 – 2719
Km_1/Vm_1 AP	mean ± sd	5.6 ± 5.0	27 ± 37	268 ± 349	301 ± 172
	range	1 – 17	0.6 – 106	12 – 1180	14 – 594

Table 4. Range of different potential specific activities calculated using Vm_1 and specific to either i) abundance of total heterotrophic prokaryotes (per cell activities), ii) heterotrophic bacterial production (per unit BP). DVF is the 'depth decreasing factor', calculated for each station as mean value in epipelagic water (SURF and DCM data) divided by the mean in deep waters (LIW and MDW) . The distribution of cell specific Vm_1 and cell specific Vm_{all} for AP and LAP are also presented on Fig 7.

enzyme	units	SURF	DCM	LIW	MDW	*DVF*
Per cell LAP	10^{-18} mol leu $bact^{-1}$ h^{-1}	0.33 – 1.52	0.44 – 2.18	0.11-0.70	0.13 – 0.54	*1.3 – 9.6*
Per cell βGLU	10^{-18} mol glucose $bact^{-1}$ h^{-1}	0.02 – 0.11	0.02 – 0.17	nd	nd	*nd*
Per cell AP	10^{-18} mole P $bact^{-1}$ h^{-1}	0.45 – 26	0.11 – 32	0.13-11	0.17-23	*0.1 – 28*
Per cell BP	10^{-18}g C $bact^{-1}$ h^{-1}	46 – 136	25 – 60	3 – 17	1 – 14	*4 – 23*
per BP LAP	nmol AA nmol C^{-1}	0.04 – 0.24	0.12 – 0.44	0.21 – 1.08	0.36 – 3.03	*0.09 – 0.76*
per BP βGLU	nmol glucose nmol C^{-1}	0.003 – 0.017	0.007 – 0.034	nd	nd	*nd*
per BP AP	nmol P nmol C^{-1}	0.09 – 2.3	0.05 – 11	0.46 – 8	0.6-40	*0.04 – 1.7*

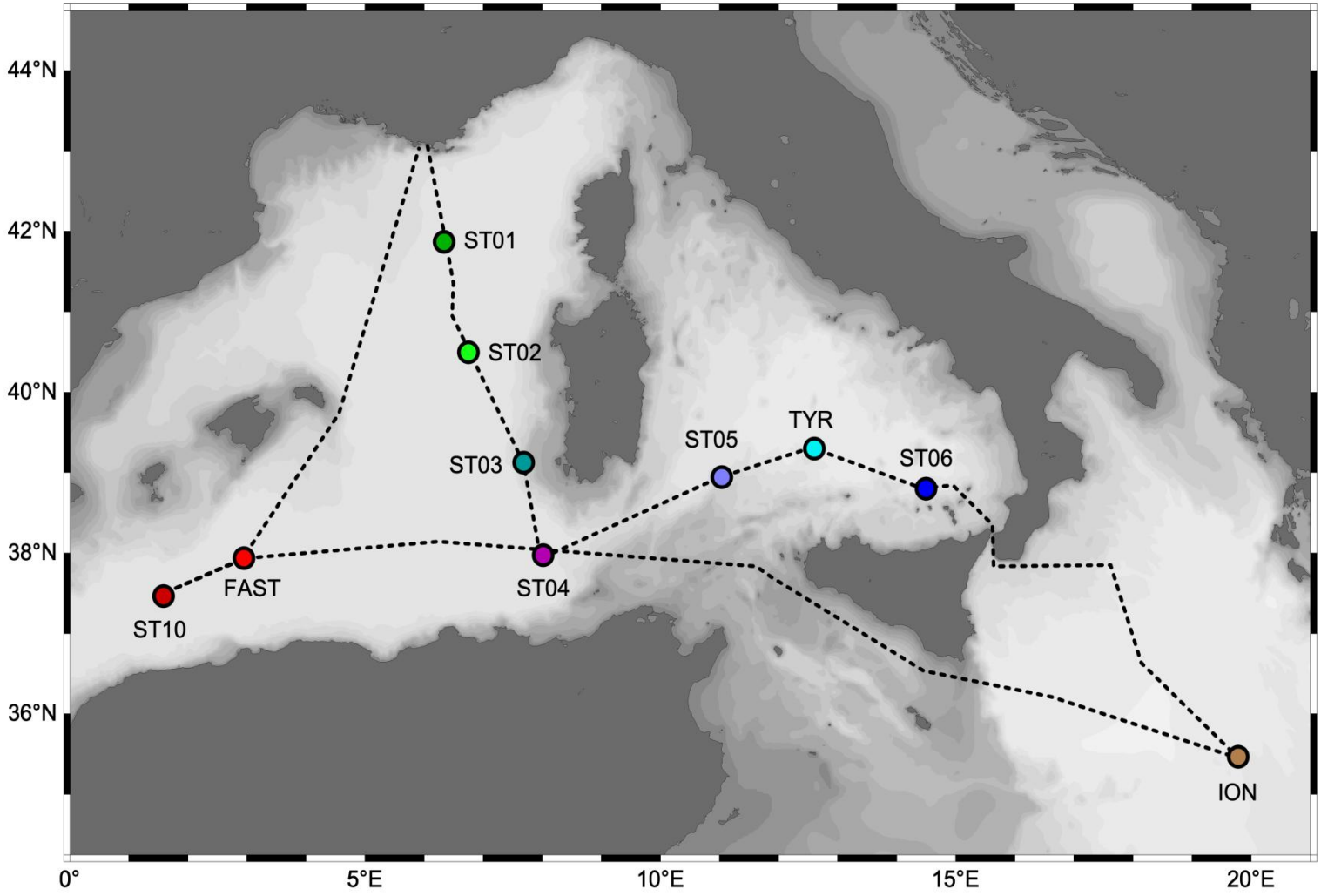
44°N
42°N
40°N
38°N
36°N
0°
5°E
10°E
15°E
20°E
ST01
ST02
ST03
ST04
ST05
TYR
ST06
FAST
ST10
ION

Fig 1

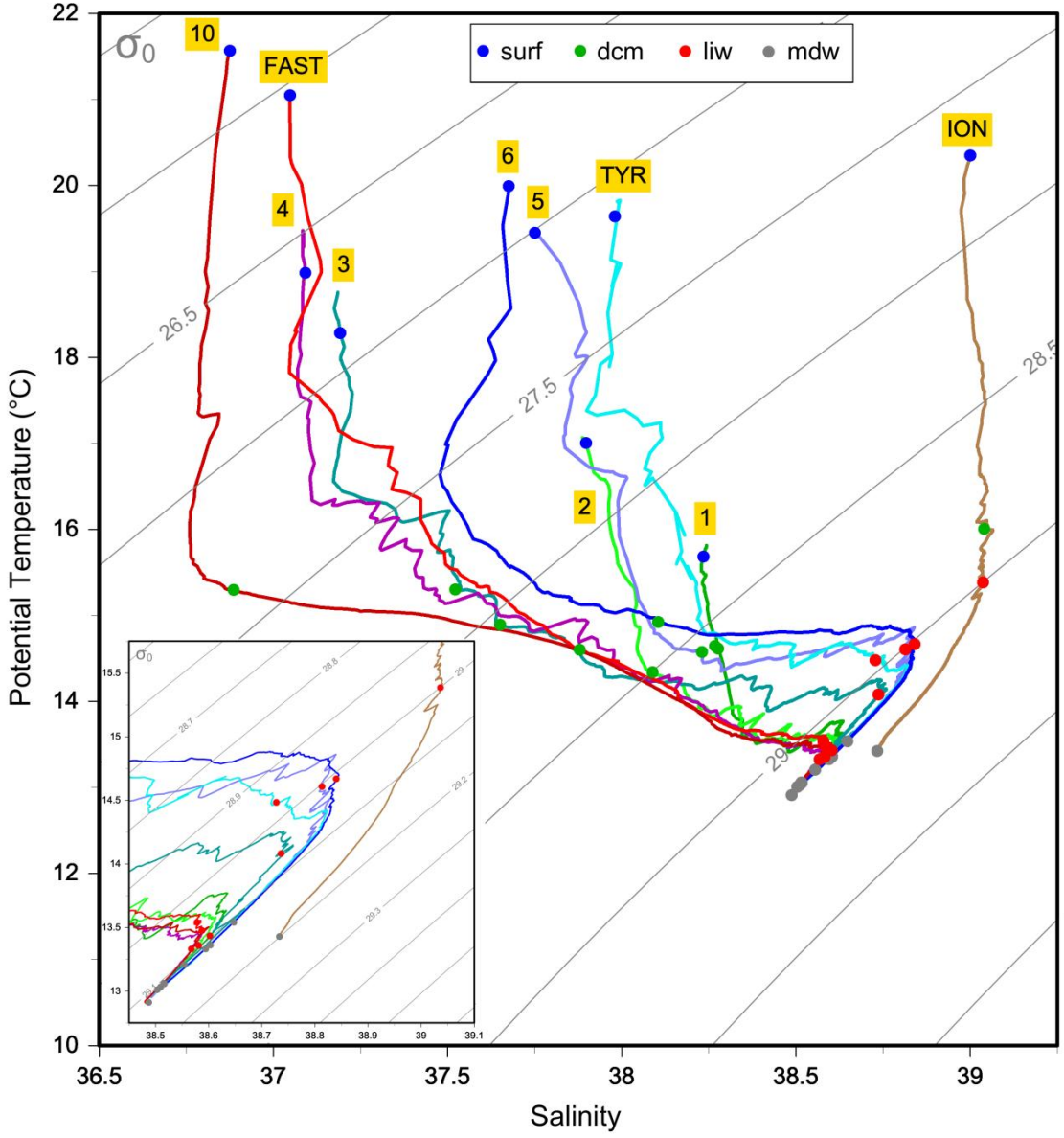
σ0
surf
dcm
liw
mdw
10
FAST
4
3
6
5
TYR
ION
2
1
26.5
27.5
28.5
Potential Temperature (°C)
Salinity
22
20
18
16
14
12
10
36.5
37
37.5
38
38.5
39

Fig 2

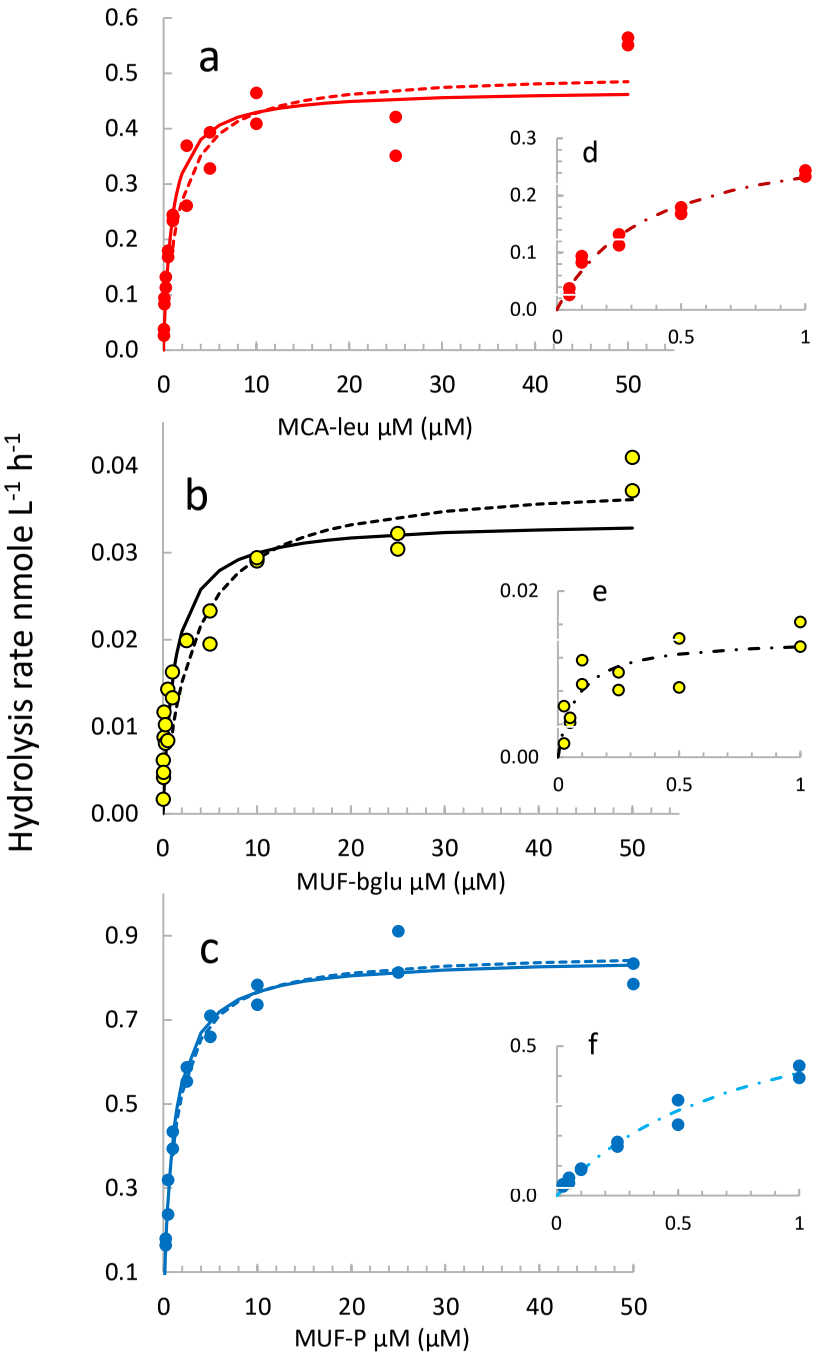
a
b
c
d
e
f
Hydrolysis rate nmole L-1 h-1
MCA-leu µM (µM)
MUF-bglu µM (µM)
MUF-P µM (µM)

Fig 3

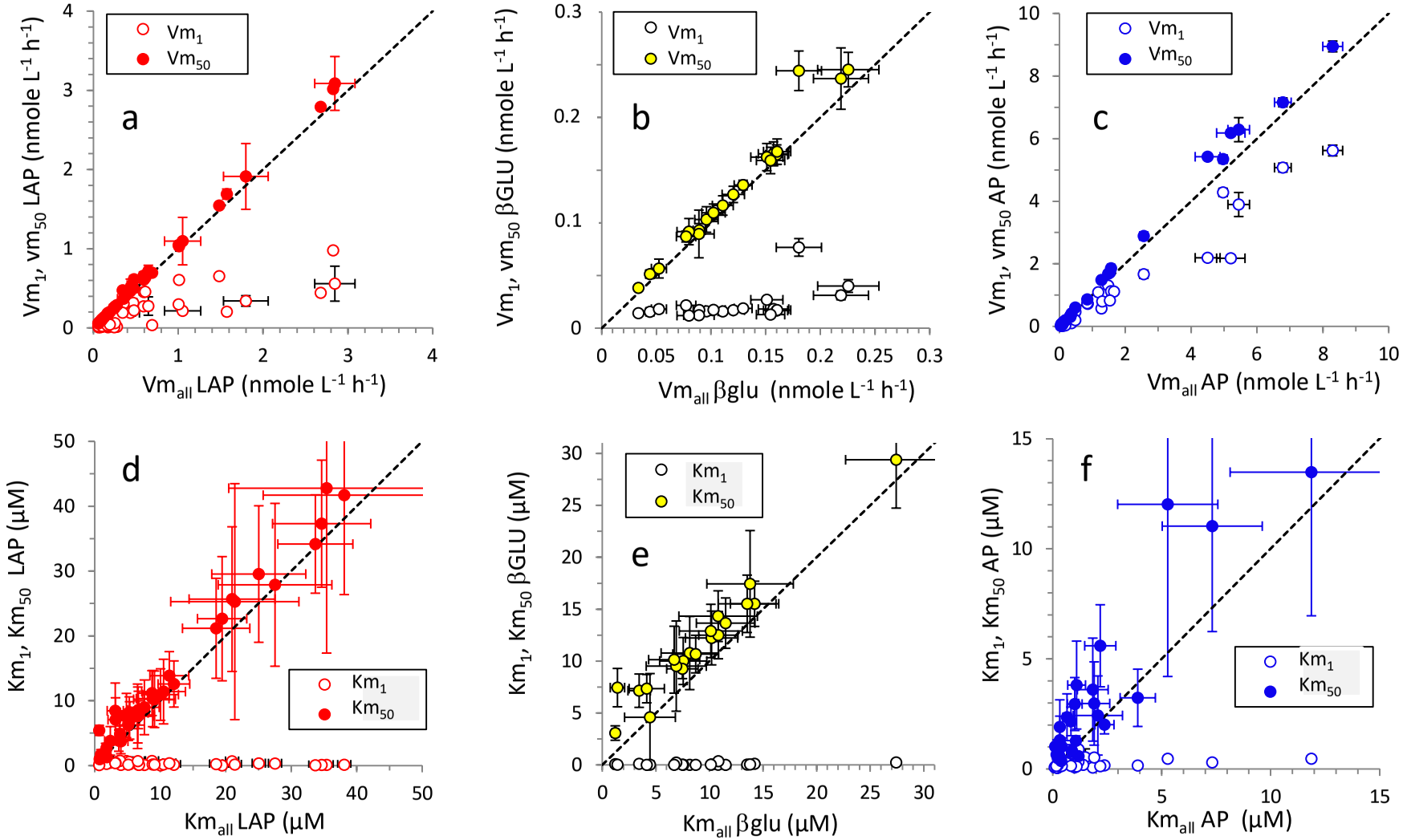
a
Vm1
Vm50
Vm1, vm50 LAP (nmole L-1 h-1)
Vmall LAP (nmole L-1 h-1)
b
Vm1
Vm50
Vm1, vm50 βGLU (nmole L-1 h-1)
Vmall βglu (nmole L-1 h-1)
c
Vm1
Vm50
Vm1, vm50 AP (nmole L-1 h-1)
Vmall AP (nmole L-1 h-1)
d
Km1
Km50
Km1, Km50 LAP (μM)
Kmall LAP (μM
e
Km1
Km50
Km1, Km50 βGLU (μM)
Kmall βglu (μM)
f
Km1
Km50
Km1, Km50 AP (μM)
Kmall AP (μM)

Fig 4

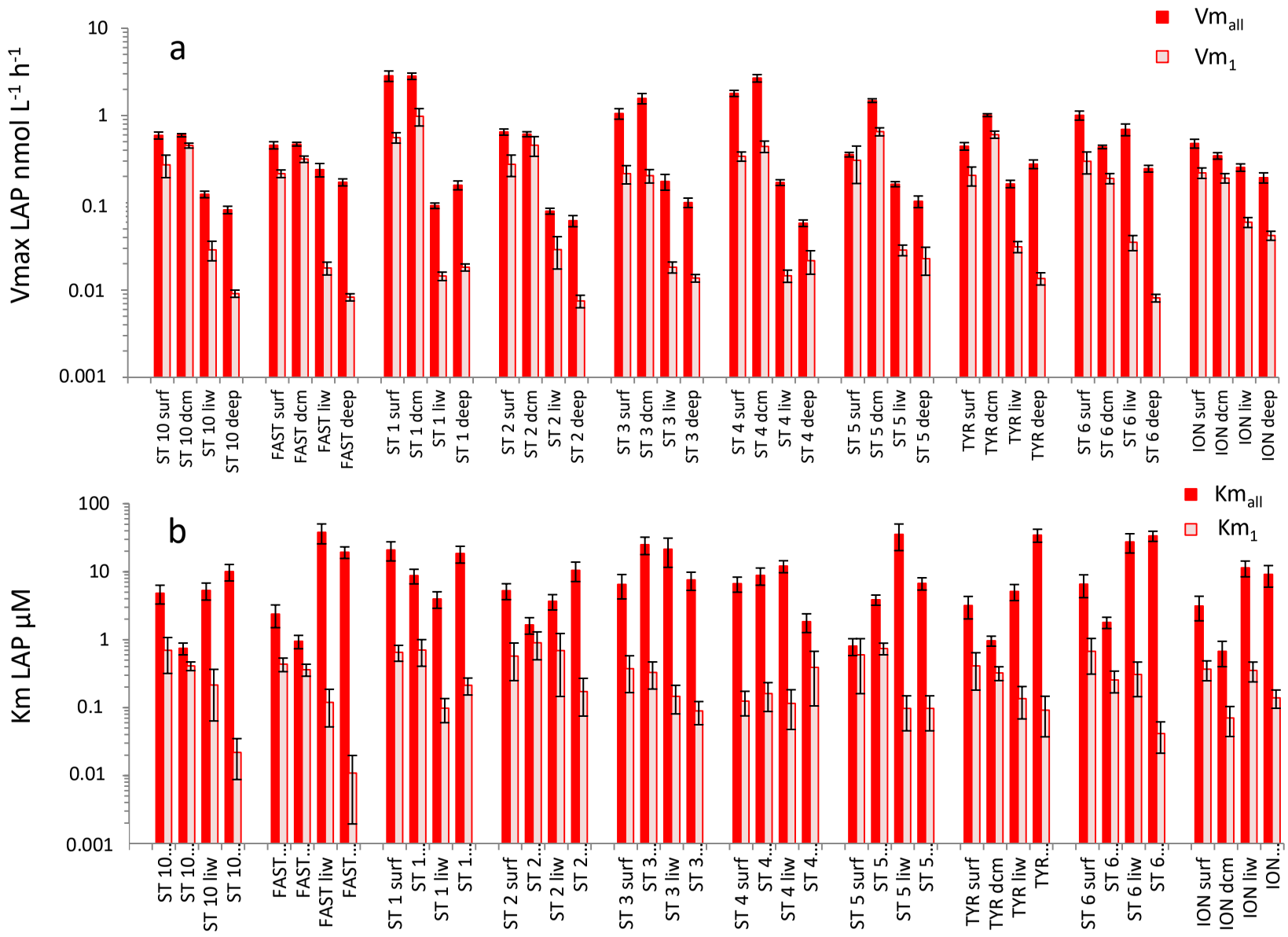
a
Vmax LAP nmol L-1 h-1
10
1
0.1
0.01
0.001
Vmall
Vm1
ST 10 surf
ST 10 dcm
ST 10 liw
ST 10 deep
FAST surf
FAST dcm
FAST liw
FAST deep
ST 1 surf
ST 1 dcm
ST 1 liw
ST 1 deep
ST 2 surf
ST 2 dcm
ST 2 liw
ST 2 deep
ST 3 surf
ST 3 dcm
ST 3 liw
ST 3 deep
ST 4 surf
ST 4 dcm
ST 4 liw
ST 4 deep
ST 5 surf
ST 5 dcm
ST 5 liw
ST 5 deep
TYR surf
TYR dcm
TYR liw
TYR deep
ST 6 surf
ST 6 dcm
ST 6 liw
ST 6 deep
ION surf
ION dcm
ION liw
ION deep
b
Km LAP µM
100
10
1
0.1
0.01
0.001
Kmall
Km1

Fig 5

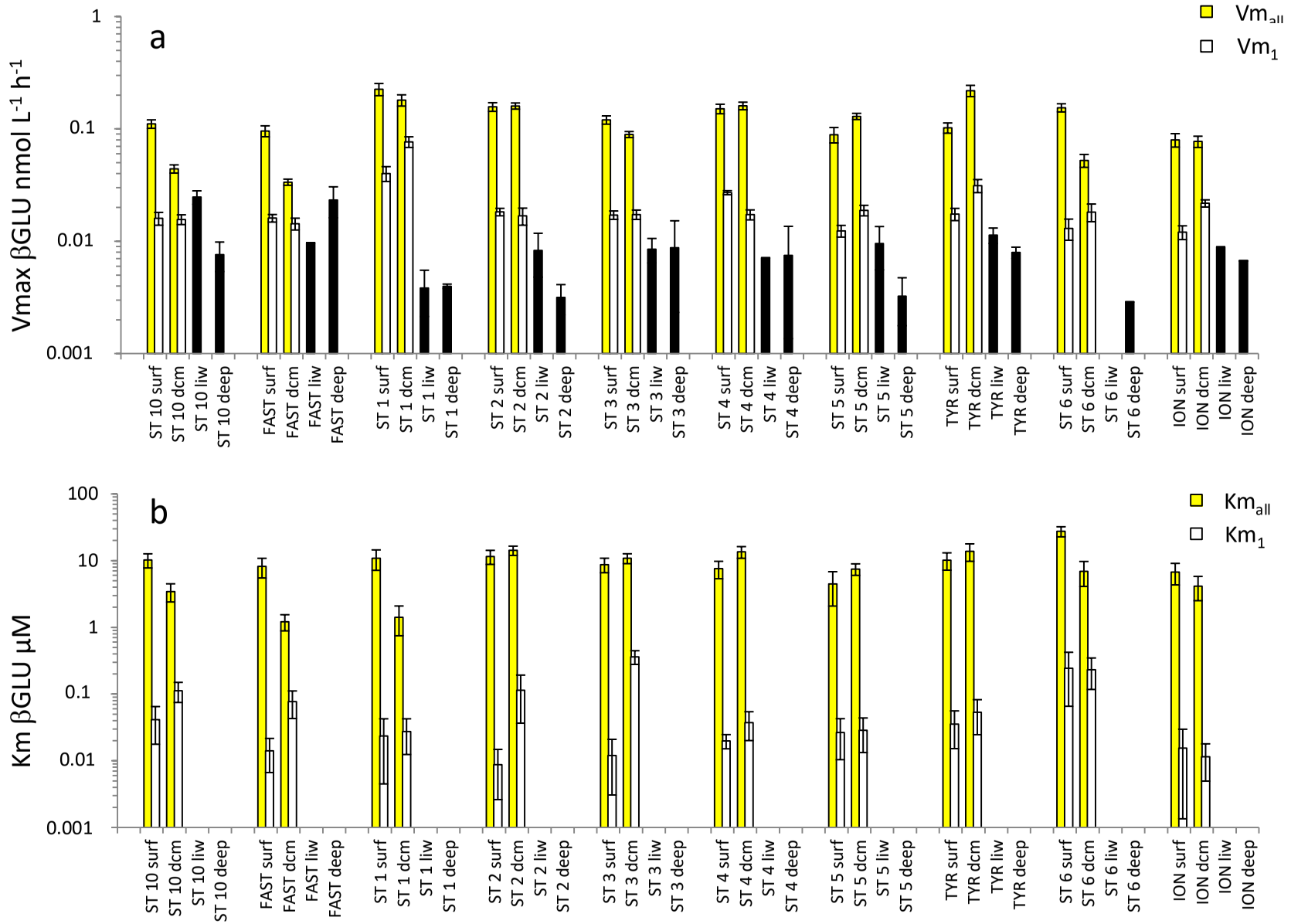
a
Vmax βGLU nmol L-1 h-1
1
0.1
0.01
0.001
Vmall
Vm1
b
Km βGLU µM
100
10
1
0.1
0.01
0.001
Kmall
Km1
ST 10 surf
ST 10 dcm
ST 10 liw
ST 10 deep
FAST surf
FAST dcm
FAST liw
FAST deep
ST 1 surf
ST 1 dcm
ST 1 liw
ST 1 deep
ST 2 surf
ST 2 dcm
ST 2 liw
ST 2 deep
ST 3 surf
ST 3 dcm
ST 3 liw
ST 3 deep
ST 4 surf
ST 4 dcm
ST 4 liw
ST 4 deep
ST 5 surf
ST 5 dcm
ST 5 liw
ST 5 deep
TYR surf
TYR dcm
TYR liw
TYR deep
ST 6 surf
ST 6 dcm
ST 6 liw
ST 6 deep
ION surf
ION dcm
ION liw
ION deep

Fig 6

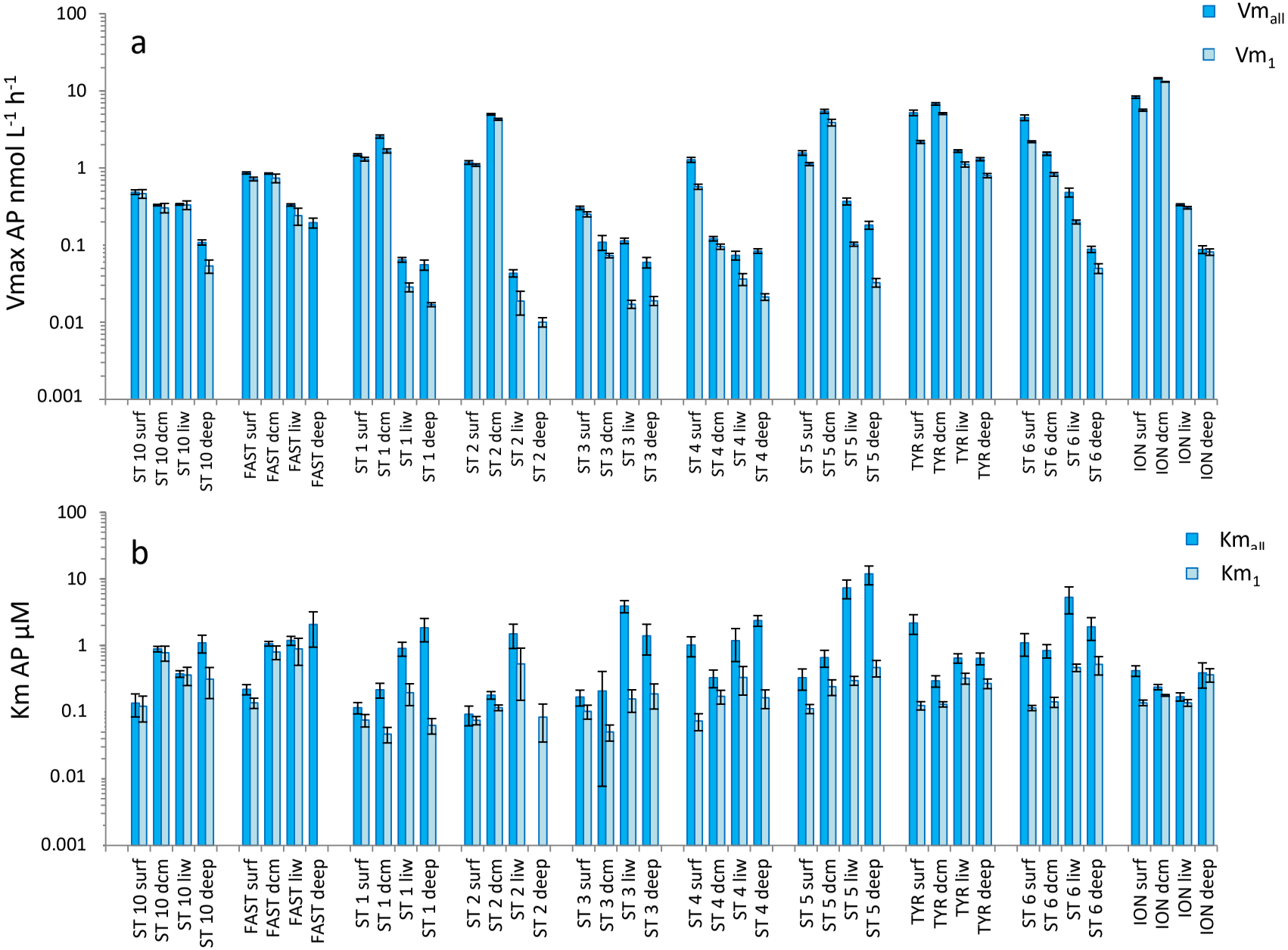
a
Vmax AP nmol L-1 h-1
100
10
1
0.1
0.01
0.001
Vmall
Vm1
ST 10 surf
ST 10 dcm
ST 10 liw
ST 10 deep
FAST surf
FAST dcm
FAST liw
FAST deep
ST 1 surf
ST 1 dcm
ST 1 liw
ST 1 deep
ST 2 surf
ST 2 dcm
ST 2 liw
ST 2 deep
ST 3 surf
ST 3 dcm
ST 3 liw
ST 3 deep
ST 4 surf
ST 4 dcm
ST 4 liw
ST 4 deep
ST 5 surf
ST 5 dcm
ST 5 liw
ST 5 deep
TYR surf
TYR dcm
TYR liw
TYR deep
ST 6 surf
ST 6 dcm
ST 6 liw
ST 6 deep
ION surf
ION dcm
ION liw
ION deep
b
Km AP µM
100
10
1
0.1
0.01
0.001
Kmall
Km1
ST 10 surf
ST 10 dcm
ST 10 liw
ST 10 deep
FAST surf
FAST dcm
FAST liw
FAST deep
ST 1 surf
ST 1 dcm
ST 1 liw
ST 1 deep
ST 2 surf
ST 2 dcm
ST 2 liw
ST 2 deep
ST 3 surf
ST 3 dcm
ST 3 liw
ST 3 deep
ST 4 surf
ST 4 dcm
ST 4 liw
ST 4 deep
ST 5 surf
ST 5 dcm
ST 5 liw
ST 5 deep
TYR surf
TYR dcm
TYR liw
TYR deep
ST 6 surf
ST 6 dcm
ST 6 liw
ST 6 deep
ION surf
ION dcm
ION liw
ION deep

Fig 7

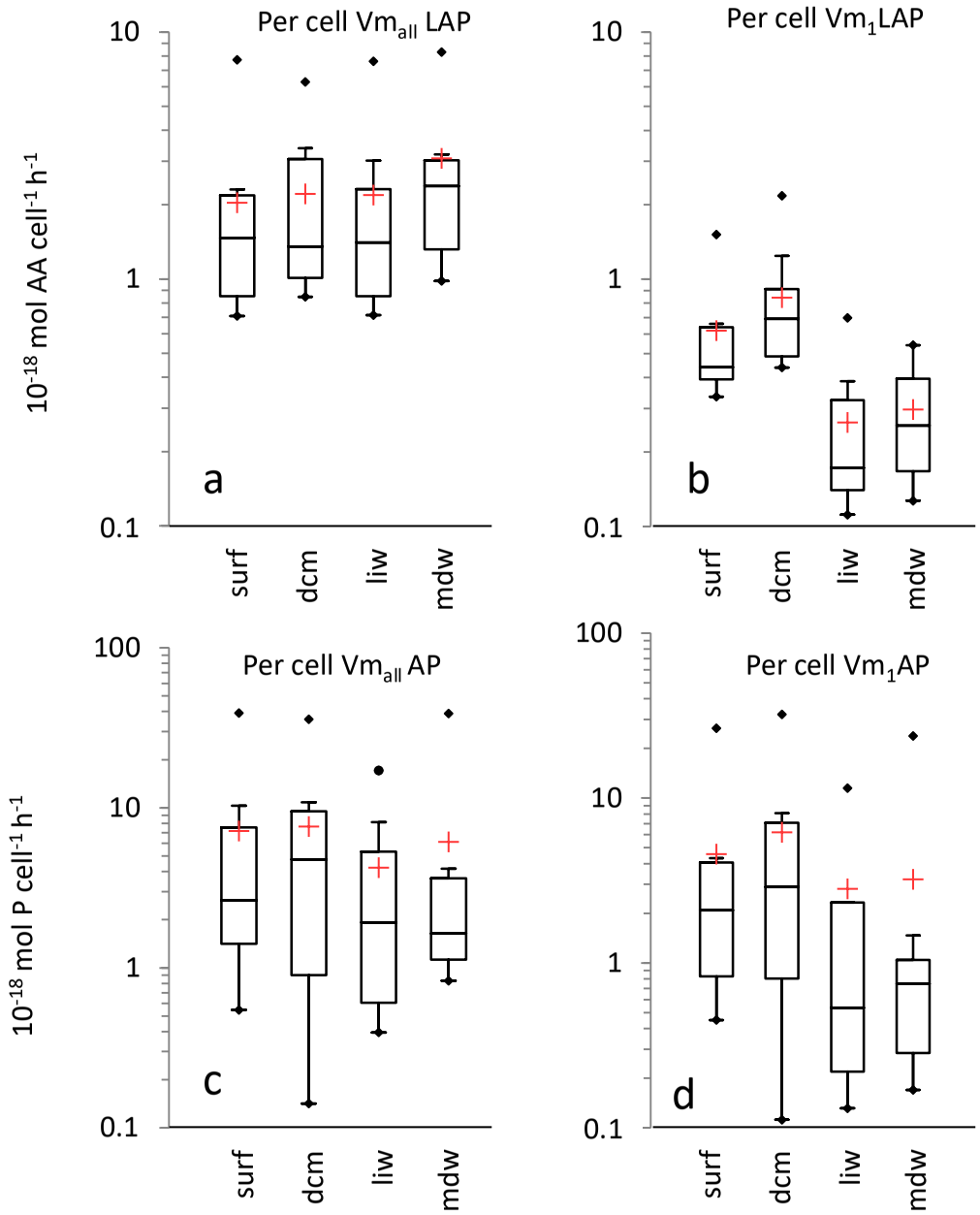
Per cell Vm$_{all}$ LAP
Per cell Vm$_1$LAP
Per cell Vm$_{all}$ AP
Per cell Vm$_1$AP
10^{-18} mol AA cell^{-1} h^{-1}
10^{-18} mol P cell^{-1} h^{-1}
10
1
0.1
100
a
b
c
d
surf
dcm
liw
mdw

Fig 8

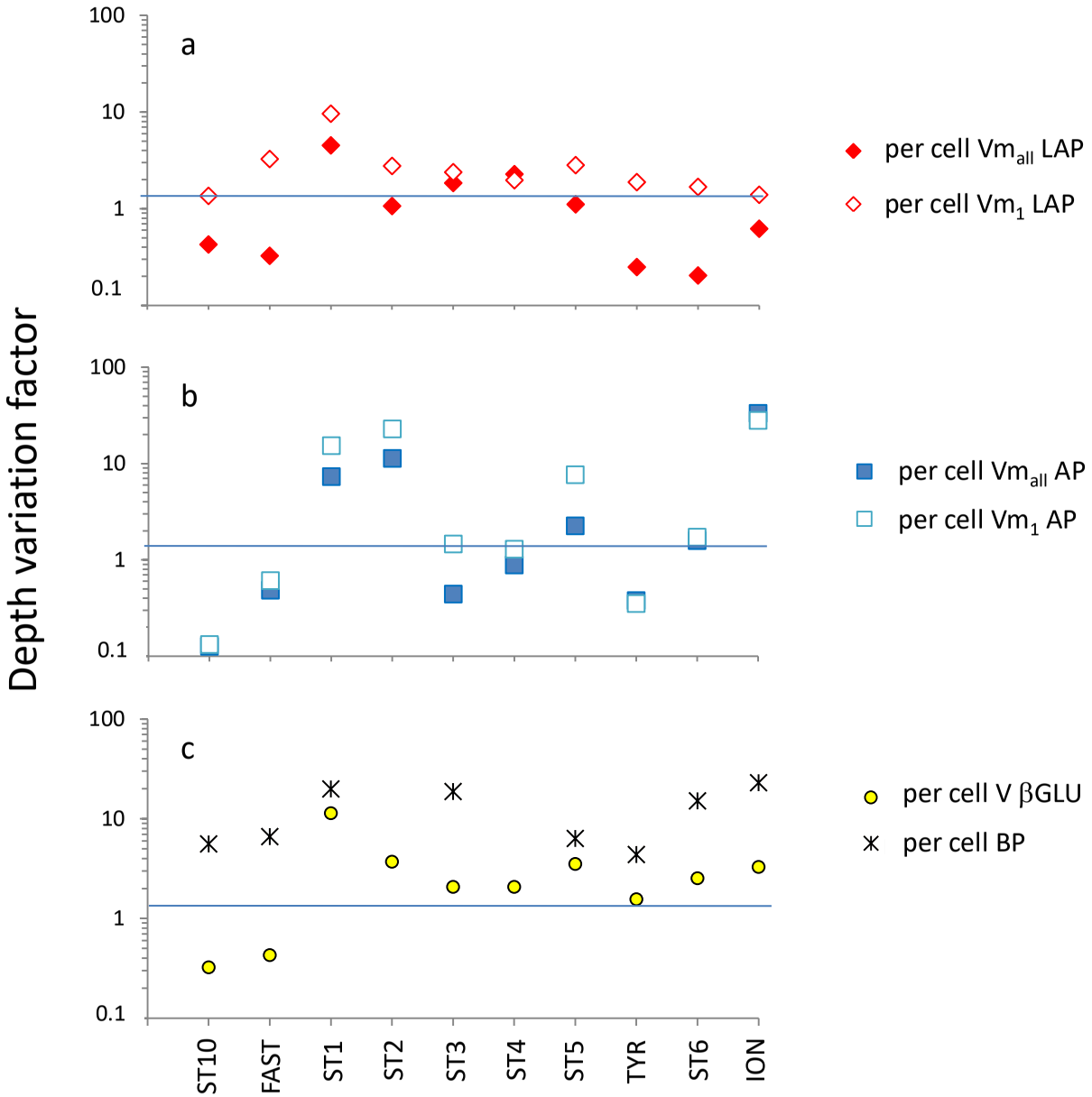
Depth variation factor
100
10
1
0.1
a
b
c
per cell Vm$_{all}$ LAP
per cell Vm$_1$ LAP
per cell Vm$_{all}$ AP
per cell Vm$_1$ AP
per cell V βGLU
per cell BP
ST10
FAST
ST1
ST2
ST3
ST4
ST5
TYR
ST6
ION

Fig 9

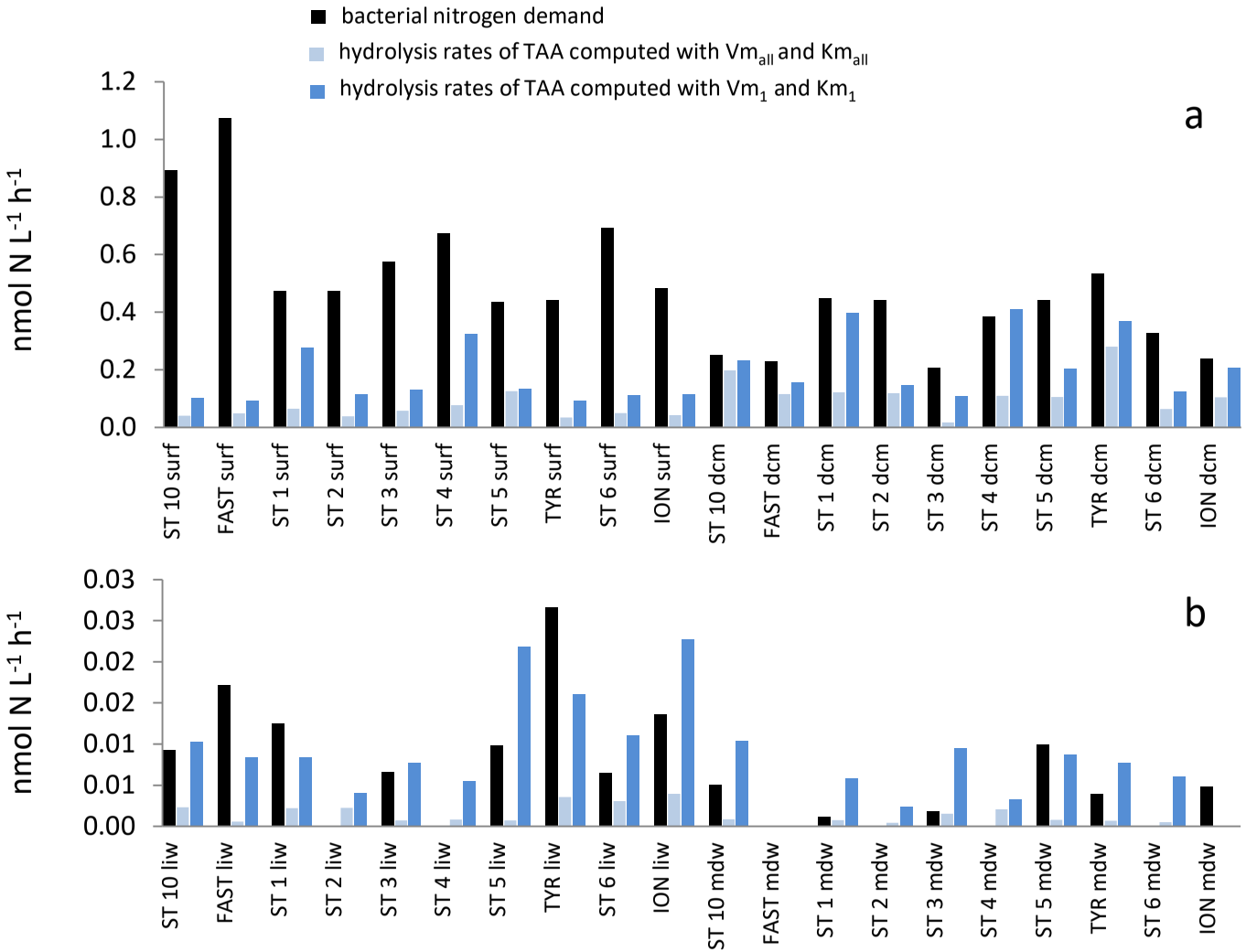
bacterial nitrogen demand
hydrolysis rates of TAA computed with Vm_{all} and Km_{all}
hydrolysis rates of TAA computed with Vm_1 and Km_1
a
b
nmol N L^{-1} h^{-1}
1.2
1.0
0.8
0.6
0.4
0.2
0.0
0.03
0.03
0.02
0.02
0.01
0.01
0.00
ST 10 surf
FAST surf
ST 1 surf
ST 2 surf
ST 3 surf
ST 4 surf
ST 5 surf
TYR surf
ST 6 surf
ION surf
ST 10 dcm
FAST dcm
ST 1 dcm
ST 2 dcm
ST 3 dcm
ST 4 dcm
ST 5 dcm
TYR dcm
ST 6 dcm
ION dcm
ST 10 liw
FAST liw
ST 1 liw
ST 2 liw
ST 3 liw
ST 4 liw
ST 5 liw
TYR liw
ST 6 liw
ION liw
ST 10 mdw
FAST mdw
ST 1 mdw
ST 2 mdw
ST 3 mdw
ST 4 mdw
ST 5 mdw
TYR mdw
ST 6 mdw
ION mdw

Fig 10

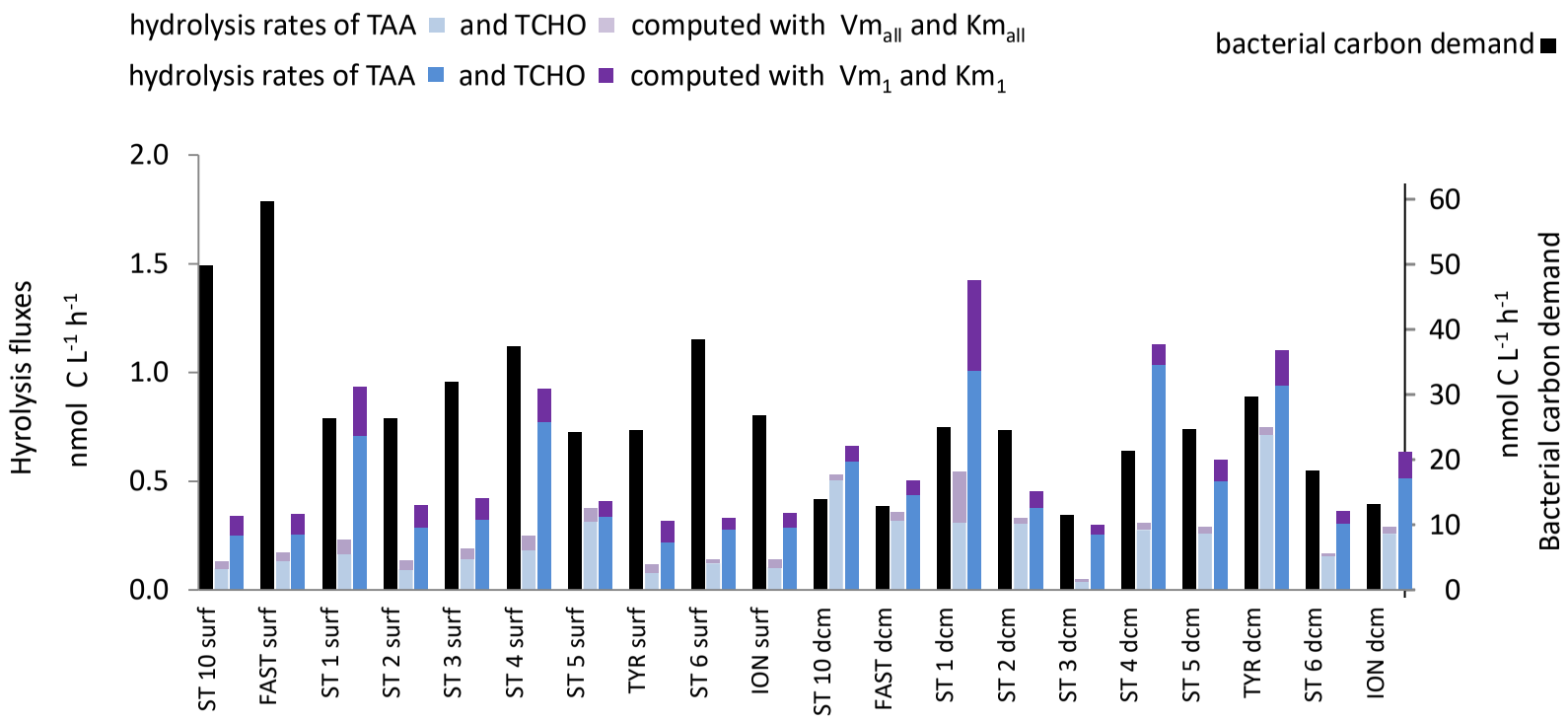
hydrolysis rates of TAA and TCHO computed with Vm$_{all}$ and Km$_{all}$
hydrolysis rates of TAA and TCHO computed with Vm$_1$ and Km$_1$
bacterial carbon demand
Hyrolysis fluxes
nmol C L^{-1} h^{-1}
Bacterial carbon demand
nmol C L^{-1} h^{-1}
2.0
1.5
1.0
0.5
0.0
60
50
40
30
20
10
0
ST 10 surf
FAST surf
ST 1 surf
ST 2 surf
ST 3 surf
ST 4 surf
ST 5 surf
TYR surf
ST 6 surf
ION surf
ST 10 dcm
FAST dcm
ST 1 dcm
ST 2 dcm
ST 3 dcm
ST 4 dcm
ST 5 dcm
TYR dcm
ST 6 dcm
ION dcm

Fig 11